

Unified study of $J/\psi \rightarrow PV$, $P\gamma^{(*)}$ and light hadron radiative processes

Yun-Hua Chen^{a,*}, Zhi-Hui Guo^{b,c,†} and Bing-Song Zou^{a,c,‡}

^a *Institute of High Energy Physics, CAS,*

Beijing 100049, People's Republic of China

^b *Department of Physics, Hebei Normal University,*

Shijiazhuang 050024, People's Republic of China

^c *State Key Laboratory of Theoretical Physics, Institute of Theoretical Physics,*

CAS, Beijing 100190, People's Republic of China

Within the framework of the effective Lagrangian approach, we perform a thorough analysis of the $J/\psi \rightarrow P\gamma(\gamma^*)$, $J/\psi \rightarrow VP$, $V \rightarrow P\gamma(\gamma^*)$, $P \rightarrow V\gamma(\gamma^*)$ and $P \rightarrow \gamma\gamma(\gamma^*)$ processes, where V stand for light vector resonances, P stand for light pseudoscalar mesons, and γ^* subsequently decays into lepton pairs. The processes with light pseudoscalar mesons η and η' are paid special attention to and the two-mixing-angle scheme is employed to describe their mixing. The four mixing parameters both in singlet-octet and quark-flavor bases are updated in this work. We confirm that the $J/\psi \rightarrow \eta(\eta')\gamma^{(*)}$ processes are predominantly dominated by the $J/\psi \rightarrow \eta_c\gamma^* \rightarrow \eta(\eta')\gamma^{(*)}$ mechanism. Predictions for the $J/\psi \rightarrow P\mu^+\mu^-$ are presented. A detailed discussion on the interplay between electromagnetic and strong transitions in the $J/\psi \rightarrow VP$ decays is given.

PACS numbers: 12.39.-x, 13.25.Gv, 13.20.Gd, 11.30.Hv

Keywords: Phenomenological models, J/ψ decays

I. INTRODUCTION

The vast decay modes of the J/ψ into light flavor hadrons provide us invaluable information on the mechanisms of light hadron production from the $c\bar{c}$ annihilation and they are also ideal for the study of light hadron dynamics, such as the $SU(3)$ -flavor symmetry breaking and Okubo-Zweig-Iizuka(OZI) rules. We focus on two types of J/ψ decays in this work, i.e. $J/\psi \rightarrow PV$ and $J/\psi \rightarrow P\gamma(\gamma^*)$, with V the light vector resonances and P the light pseudoscalar mesons.

For the charmonium radiative decays $J/\psi \rightarrow P\gamma$, the dominant underlying mechanism is the $c\bar{c}$ annihilation into two gluons plus a photon, as advocated in many previous works [1–13]. While

*chenyh@ihep.ac.cn

†Corresponding author: zhguo@mail.hebtu.edu.cn

‡zoubs@itp.ac.cn

for the $J/\psi \rightarrow PV$ decays, both electromagnetic (EM) and strong interactions will enter and an important issue is the interplay between the two parts, that has been extensively studied in literature [1–3, 14–20]. All of the attempts to understand these $J/\psi \rightarrow PV$ decays are based on the similar model with slight variations. In this model, the dominant part of the amplitude is assumed to proceed through the $c\bar{c}$ annihilation into light hadrons via three gluons, which is the so-called the single-OZI suppressed diagram. Later on, doubly OZI suppressed diagrams are also introduced, where an additional gluon is exchanged between the vector and pseudoscalar mesons. For the EM interaction pieces, there are also two different kinds of diagrams, the singly disconnected one (one photon exchange) and doubly disconnected ones. We refer to Ref. [1] for a detailed discussion on different mechanisms. Based on these arguments, the previous research works, such as those in Refs. [1–3, 14–20], proceed the discussion through directly writing down the amplitudes by introducing some phenomenological couplings for different processes. The $SU(3)$ symmetry breaking effects are also introduced at the amplitude level.

In this work, we do not follow the previous routine to further scrutinize and refine different terms in the amplitudes, instead we start from the very beginning by constructing the relevant effective Lagrangians and then use them to calculate the amplitudes. One of the advantages starting from the effective Lagrangian approach is that it allows us to make a systematic study of different processes by simultaneously taking into account different mechanisms in a consistent and transparent way. This approach is specially useful to incorporate the OZI rule and $SU(3)$ -flavor breaking effects.

The only theoretical framework that is generally accepted to account for the successful OZI rule in various hadronic processes is the large N_C QCD [21]. It has been demonstrated in Ref. [22] that one can build a simple relation between the number of flavor traces in effective field theory and the N_C counting rule, though some care should be paid attention to in special cases due to the subtlety of using matrix relations among the traces of products [22]. Generally speaking, to introduce one additional trace to an operator in the effective Lagrangian will make this operator one more order suppressed by $1/N_C$, i.e. one more order of OZI suppression. Therefore, it is convenient and easy to systematically include the OZI suppressed effects in the effective Lagrangian approach. Another important benefit to work in the effective Lagrangian framework for the processes of J/ψ decaying into light hadrons is to properly incorporate the $SU(3)$ -flavor symmetry breaking effects. In the chiral limit, QCD exhibits the strict $SU(3)_L \times SU(3)_R \rightarrow SU(3)_V$ spontaneous-symmetry-breaking pattern, leading to eight massless pseudo Nambu-Goldstone bosons (pNGBs), which obey an exact $SU(3)$ symmetry. This exact $SU(3)$ -flavor symmetry has to be broken in order to be consistent

with the small but non-vanishing masses of π, K, η . The strong $SU(3)$ -flavor symmetry breaking in QCD is implemented through the introduction of explicit non-vanishing quark masses. This feature of QCD is elegantly embedded in chiral perturbation theory (χ PT) [22] through the chiral building block operators χ_{\pm} , which we will explain in detail later. Apparently the chiral power counting is by no means applied to the pNGBs in J/ψ decays, since the momenta of pNGBs are far beyond the validity region allowed by χ PT. Nevertheless even we do not have the chiral power counting, other ingredients from chiral effective field theory can be still useful for us to construct the relevant effective Lagrangian for J/ψ decays into light hadrons, such as the well-established chiral building blocks incorporating the light pNGBs and the systematic way to consider the $1/N_C$ or OZI suppressed and $SU(3)$ symmetry breaking effects.

In addition to the light pNGBs, we also need to include the dynamical fields of light vector resonances. Guided by chiral symmetry and large N_C expansion, resonance chiral theory ($R\chi T$) [23] provides us a reliable theoretical framework to study the interaction between the light flavor resonances and pNGBs in the intermediate energy region and it has been successfully applied in many phenomenological processes [24–32]. The building blocks involving resonance states from $R\chi T$ [23] will be also employed in our present work to construct the relevant effective Lagrangian describing the interactions between light hadrons and the J/ψ . These Lagrangians offer an efficient and systematic framework to analyze the processes of $J/\psi \rightarrow P\gamma$, $J/\psi \rightarrow VP$ and $J/\psi \rightarrow Pl^+l^-$, with the leptons $l = e, \mu$.

From the experimental point of view, the first measurements of $J/\psi \rightarrow P\gamma^* \rightarrow Pe^+e^-$ ($P = \pi^0, \eta, \eta'$) are performed by the BESIII collaboration very recently [33] and updated world average results for $J/\psi \rightarrow PV$ and $P\gamma$ are available [34] as well. These new measurements and updated experimental results will be definitely useful to pin down the unknown couplings in our theoretical model and hence to reveal the underlying mechanisms of J/ψ decays into light hadrons. For $J/\psi \rightarrow \eta e^+e^-$ and $J/\psi \rightarrow \eta' e^+e^-$, the vector-dominant-model (VMD) predictions of the decay rates are consistent with the experimental data. While there are around 2.5 standard deviations between the theoretical prediction and the measurement for $J/\psi \rightarrow \pi^0 e^+e^-$ process, which deserves further study [13].

Another important issue we will address in this article is the properties of η and η' mesons. The composition of the η and η' mesons has long been a subject of theoretical discussions [3, 35–37] and is of current interest with many new measurements with high statistics and high precision [38–40]. In Ref. [41], the two-mixing-angle description has been proposed to settle the $\eta - \eta'$ mixing, going beyond the conventional one-mixing-angle description [37]. The robustness of the two-mixing-

angle description scheme has been confirmed in various analyses [2, 8, 9, 15, 30, 42–47], and we have provided a mini-review on the $\eta - \eta'$ mixing in Ref. [30]. In this article, we extend the previous work of Ref. [30] by including the J/ψ decays: $J/\psi \rightarrow P\gamma$, $J/\psi \rightarrow VP$, $J/\psi \rightarrow Pe^+e^-$, the form factors of $J/\psi \rightarrow \eta'\gamma^*$, in addition to the processes with only light flavor hadrons, such as $P \rightarrow V\gamma$, $V \rightarrow P\gamma$, $P \rightarrow \gamma\gamma$, $P \rightarrow \gamma l^+ l^-$, $V \rightarrow Pl^+ l^-$, as well as the form factors of $\eta \rightarrow \gamma\gamma^*$, $\eta' \rightarrow \gamma\gamma^*$, $\phi \rightarrow \eta\gamma^*$.

This paper is organized as follows. In Sec. II, we introduce the theoretical framework and elaborate the calculations for the transition amplitudes of $J/\psi \rightarrow P\gamma^*$ and $J/\psi \rightarrow VP$. In Sec. III, we present the fit results and discuss the interplay between different mechanisms in J/ψ decays. Summary and conclusions are given in Sec. IV.

II. THEORETICAL FRAMEWORK

A. The relevant Lagrangian of J/ψ hadronic decays

We will simultaneously study the J/ψ decaying into light hadrons and the light meson radiative decays. Therefore two different types of effective Lagrangians, i.e. the ones involving interactions between J/ψ and light hadrons, and those only including interactions between light-hadron themselves, need to be constructed. The latter have been discussed in detail in Ref. [30] and we simply introduce them below for completeness.

For the interaction operators between J/ψ and light hadrons, we construct the effective Lagrangian by taking the basic building blocks involving light hadron states from χ PT [22] and $R\chi$ T [23]. A subtlety about the description of vector resonances in $R\chi$ T should be pointed out. The vector resonances are described in the antisymmetry tensor representation [22, 23], not in the conventional Proca field formalism. The reason behind is that with the vector resonances in the antisymmetric tensor representation, one can collect, upon integrating out the heavy resonance states, the bulk of low energy constants in χ PT without including the additional local counterterms [48]. Therefore we will use the antisymmetric tensor formalism to describe the light vector resonances, as we did in Ref. [30]. While for the J/ψ , we will simply use the Proca field formalism in order to reduce the number of free couplings.

In order to set up the notations, we introduce the effective Lagrangian only involving light hadrons first. In the large N_C limit, the $U_A(1)$ anomaly from QCD is suppressed so that the singlet η_0 meson becomes the ninth pNGB and can be systematically incorporated into the $U(3)$

chiral Lagrangian [49–51]. We use the exponential realization for $U(3)_L \times U(3)_R/U(3)_V$ coset coordinates

$$\tilde{U} = \tilde{u}^2 = e^{i\frac{\sqrt{2}\Phi}{F}}, \quad (1)$$

where the pNGB octet plus singlet are given by

$$\Phi = \begin{pmatrix} \frac{1}{\sqrt{2}}\pi^0 + \frac{1}{\sqrt{6}}\eta_8 + \frac{1}{\sqrt{3}}\eta_0 & \pi^+ & K^+ \\ \pi^- & -\frac{1}{\sqrt{2}}\pi^0 + \frac{1}{\sqrt{6}}\eta_8 + \frac{1}{\sqrt{3}}\eta_0 & K^0 \\ K^- & \bar{K}^0 & -\frac{2}{\sqrt{6}}\eta_8 + \frac{1}{\sqrt{3}}\eta_0 \end{pmatrix}. \quad (2)$$

The basic building blocks involving the pNGBs and external source fields read

$$\begin{aligned} \tilde{u}_\mu &= i\tilde{u}^\dagger D_\mu \tilde{U} \tilde{u}^\dagger = i\{\tilde{u}^\dagger(\partial_\mu - ir_\mu)\tilde{u} - \tilde{u}(\partial_\mu - \tilde{u}\ell_\mu)\tilde{u}^\dagger\}, \\ \tilde{\chi}_\pm &= \tilde{u}^\dagger \chi \tilde{u}^\dagger \pm \tilde{u} \chi^\dagger \tilde{u}, \quad \tilde{f}_\pm^{\mu\nu} = \tilde{u} F_L^{\mu\nu} \tilde{u}^\dagger \pm \tilde{u}^\dagger F_R^{\mu\nu} u, \end{aligned} \quad (3)$$

where $\chi = 2B_0(s + ip)$ incorporates the pseudoscalar (p) and scalar (s) external sources. $F_L^{\mu\nu}$ and $F_R^{\mu\nu}$ are the field-strength tensors for the left and right external sources, respectively. All of the building blocks $X = \tilde{u}_\mu, \tilde{\chi}_\pm, \tilde{f}_\pm^{\mu\nu}$ in Eq. (3) then transform under the chiral group transformations as

$$X \rightarrow hXh^\dagger, \quad h \in U(3)_V. \quad (4)$$

Notice that we have introduced the tildes to the objects involving the pNGB nonet in order to distinguish those with octet from $SU(3)$ χ PT. In the following construction of effective Lagrangian with light resonances and J/ψ , the pNGB fields will enter only through the three types of building blocks presented in Eq. (3).

The $U(3)$ χ PT Lagrangian to lowest order, $O(p^2)$, is

$$\mathcal{L}_\chi^{(2)} = \frac{F^2}{4} \langle \tilde{u}_\mu \tilde{u}^\mu + \tilde{\chi}_+ \rangle + \frac{F^2}{3} M_0^2 \ln^2 \det \tilde{u}, \quad (5)$$

where the last term stands for the QCD $U_A(1)$ anomaly effect, leading to a non-vanishing mass for the η_0 field even in the chiral limit. The parameter F denotes the value of the pion decay constant $F_\pi = 92.2$ MeV in the chiral limit and B_0 in Eq. (3) is related to the quark condensate through $\langle 0 | \psi \bar{\psi} | 0 \rangle = -F^2 B_0 [1 + O(m_q)]$, with m_q the light quark mass. The explicit chiral symmetry breaking is realized in χ PT by assigning the vacuum expectation values of the scalar sources as $s = \text{Diag}\{m_u, m_d, m_s\}$. Throughout, we take $m_u = m_d$ and use the leading order relations $2m_u B_0 = m_\pi^2$ and $(m_u + m_s)B_0 = m_K^2$ [22, 52].

The physical η and η' states are from the mixing between η_8 and η_0 . Following a general discussion in $U(3)$ χ PT, the η - η' mixing should be formulated in the two-mixing-angle framework, instead of the conventional one-mixing-angle scheme [41, 53]. In the octet and singlet basis, the η - η' mixing is parameterized by [41, 53]

$$\begin{pmatrix} \eta \\ \eta' \end{pmatrix} = \frac{1}{F} \begin{pmatrix} F_8 \cos \theta_8 & -F_0 \sin \theta_0 \\ F_8 \sin \theta_8 & F_0 \cos \theta_0 \end{pmatrix} \begin{pmatrix} \eta_8 \\ \eta_0 \end{pmatrix}, \quad (6)$$

where F_8 and F_0 denote the weak decay constants of the axial octet and singlet currents, respectively. By taking $F_8 = F_0 = F$ and $\theta_0 = \theta_8$ in Eq.(6), the conventional one-mixing-angle scheme is recovered.

Analogously, one can choose the quark-flavor basis to parameterize the η - η' mixing as

$$\begin{pmatrix} \eta \\ \eta' \end{pmatrix} = \frac{1}{F} \begin{pmatrix} F_q \cos \phi_q & -F_s \sin \phi_s \\ F_q \sin \phi_q & F_s \cos \phi_s \end{pmatrix} \begin{pmatrix} \eta_q \\ \eta_s \end{pmatrix}, \quad (7)$$

with $\eta_q = (\eta_8 + \sqrt{2}\eta_0)/\sqrt{3}$ and $\eta_s = (\eta_0 - \sqrt{2}\eta_8)/\sqrt{3}$. In this case the η_q and η_s states are generated by the axial vector currents with the quark flavors $q\bar{q} = (u\bar{u} + d\bar{d})/\sqrt{2}$ and $s\bar{s}$, respectively. Obviously the two mixing matrices from different bases in Eqs. (6) and (7) are related to each other through an orthogonal transformation. So they are equivalent to describing the η - η' mixing. If only the leading order of N_C chiral operators with quark mass corrections are considered, the $SU(3)$ breaking by quark masses will affect the η_q and η_s differently in the quark-flavor basis, and the angles ϕ_q and ϕ_s will be equal. This is the characteristic of the Feldmann-Kroll-Stech (FKS) formalism [2]. If general operators are included in the discussion, the quark-flavor basis will lose these features. Nevertheless, it seems that the phenomenological analyses support the fact that the values of ϕ_q and ϕ_s are indeed very close to each other [2, 9, 37]. In the following phenomenological discussions we will explore both mixing scenarios in the singlet-octet and quark-flavor bases.

Next we follow closely $R\chi$ T [23] to include the vector resonances. The ground multiplet of vector resonances was explicitly incorporated in the antisymmetric tensor representation in $R\chi$ T. The kinetic term of the vector resonance Lagrangian reads [23]

$$\mathcal{L}_{kin}(V) = -\frac{1}{2} \langle \nabla^\lambda V_{\lambda\mu} \nabla_\nu V^{\nu\mu} - \frac{M_V^2}{2} V_{\mu\nu} V^{\mu\nu} \rangle, \quad (8)$$

where the ground vector nonet matrix is given by

$$V_{\mu\nu} = \begin{pmatrix} \frac{1}{\sqrt{2}}\rho^0 + \frac{1}{\sqrt{6}}\omega_8 + \frac{1}{\sqrt{3}}\omega_0 & \rho^+ & K^{*+} \\ \rho^- & -\frac{1}{\sqrt{2}}\rho^0 + \frac{1}{\sqrt{6}}\omega_8 + \frac{1}{\sqrt{3}}\omega_0 & K^{*0} \\ K^{*-} & \bar{K}^{*0} & -\frac{2}{\sqrt{6}}\omega_8 + \frac{1}{\sqrt{3}}\omega_0 \end{pmatrix}_{\mu\nu}, \quad (9)$$

and the covariant derivative and the chiral connection are defined as

$$\nabla_\mu V = \partial_\mu V + [\tilde{\Gamma}_\mu, V], \quad \tilde{\Gamma}_\mu = \frac{1}{2} \{ \tilde{u}^+ (\partial_\mu - ir_\mu) \tilde{u} + \tilde{u} (\partial_\mu - il_\mu) \tilde{u}^+ \}. \quad (10)$$

The transformation laws of the resonance multiplet and its covariant derivative under chiral group transformations are the same as the building blocks in Eq. (3)

$$V \rightarrow h V h^\dagger, \quad \nabla_\mu V \rightarrow h (\nabla_\mu V) h^\dagger, \quad h \in U(3)_V. \quad (11)$$

The masses of the resonances in the ground multiplet are degenerate in Eq. (8) and their mass splitting is governed by a single resonance operator at leading order of $1/N_C$ [54]

$$- \frac{1}{2} e_m^V \langle V_{\mu\nu} V^{\mu\nu} \chi_+ \rangle. \quad (12)$$

It has demonstrated that the single operator in the previous equation can well explain the mass splittings of the ground vector resonances in Eq. (9) and can also perfectly describe the quark mass dependences of the $\rho(770)$ mass from lattice simulations [55, 56]. Therefore it is justified for us to simply use the physical masses for the vector resonances in the phenomenological discussions.

The physical states of $\omega(782)$ and $\phi(1020)$ result from the ideal mixing of ω_0 and ω_8

$$\omega_0 = \sqrt{\frac{2}{3}} \omega - \sqrt{\frac{1}{3}} \phi, \quad \omega_8 = \sqrt{\frac{2}{3}} \phi + \sqrt{\frac{1}{3}} \omega. \quad (13)$$

The transitions between the vector resonances and the photon field are described by one single operator in the minimal version of $R\chi T$ [23]

$$\mathcal{L}_2(V) = \frac{F_V}{2\sqrt{2}} \langle V_{\mu\nu} \tilde{f}_+^{\mu\nu} \rangle. \quad (14)$$

Now we construct the effective Lagrangian describing J/ψ radiative decays and J/ψ decaying to light hadrons. We use the Proca vector field to describe the J/ψ , mainly due to the consideration of reducing the number of coupling vertices. We first consider the strong interaction vertices for J/ψ decaying to a light vector and a pNGB. Three terms are introduced

$$\mathcal{L}_{\psi VP} = M_\psi h_1 \varepsilon_{\mu\nu\rho\sigma} \psi^\mu \langle \tilde{u}^\nu V^{\rho\sigma} \rangle + \frac{1}{M_\psi} h_2 \varepsilon_{\mu\nu\rho\sigma} \psi^\mu \langle \{ \tilde{u}^\nu, V^{\rho\sigma} \} \tilde{\chi}_+ \rangle + M_\psi h_3 \varepsilon_{\mu\nu\rho\sigma} \psi^\mu \langle \tilde{u}^\nu \rangle \langle V^{\rho\sigma} \rangle, \quad (15)$$

where the first term can be related to the leading three-gluon-annihilation (singly OZI disconnected) diagram proposed in Refs. [1, 3, 14–16, 18–20], the second term stands for the strong $SU(3)$ symmetry breaking term caused by the quark masses and the last one corresponds to the doubly OZI-suppressed diagram. We have introduced the M_ψ factors in Eq. (15) so that the couplings $h_{i=1,2,3}$ are dimensionless.

For the interaction vertices with J/ψ , one pNGB and one photon field, we have two operators

$$\mathcal{L}_{\psi P\gamma} = g_1 \varepsilon_{\mu\nu\rho\sigma} \psi^\mu \langle \tilde{u}^\nu \tilde{f}_+^{\rho\sigma} \rangle + \frac{1}{M_\psi^2} g_2 \varepsilon_{\mu\nu\rho\sigma} \psi^\mu \langle \{ \tilde{u}^\nu, \tilde{f}_+^{\rho\sigma} \} \tilde{\chi}_+ \rangle, \quad (16)$$

where the second term generates the $SU(3)$ -flavor symmetry breaking caused by the quark masses for the $J/\psi P\gamma$ vertices, with $P = \pi, \eta, \eta'$.

The transition between the J/ψ and the photon field is described by

$$\mathcal{L}_2^\psi = \frac{-1}{2\sqrt{2}} \frac{f_\psi}{M_\psi} \langle \hat{\psi}_{\mu\nu} \tilde{f}_+^{\mu\nu} \rangle, \quad (17)$$

with $\hat{\psi}_{\mu\nu} = \partial_\mu \psi^\nu - \partial_\nu \psi^\mu$. The coupling strength f_ψ can be determined from the decay width of $J/\psi \rightarrow e^+ e^-$:

$$f_\psi = \left(\frac{27 M_\psi \Gamma_{\psi \rightarrow e^+ e^-}}{32 \pi \alpha^2} \right)^{\frac{1}{2}}, \quad (18)$$

where the masses of electron and positron have been neglected, and $\alpha = e^2/4\pi$ stands for the fine structure constant.

The $J/\psi \rightarrow VP$ decay processes can be categorized into two classes: (i) isospin conserved channels, such as $J/\psi \rightarrow \rho\pi, \omega\eta^{(\prime)}, \phi\eta^{(\prime)}, K^*\bar{K}$, which include both strong and EM transitions; (ii) isospin violated channels, such as $J/\psi \rightarrow \rho\eta^{(\prime)}, \omega\pi^0$, of which the leading contribution is the EM transition. In Fig. 1, we show the four types of diagrams that contribute to the $J/\psi \rightarrow VP$ decays, where the diagram (a) represents the strong interactions from the Lagrangian in Eq. (15), and the remaining diagrams (b-d) depict the EM interactions. The solid square denotes the mixing between η_c and $\eta(\eta')$, which will be addressed in the following section. The open circle in the diagram (d) of Fig. 1 stands for the radiative transition amplitudes of the pNGBs and light vector resonances, which have been the focus in our previous work in Ref. [30]. We will directly take these amplitudes from the former reference. For the sake of completeness, we simply show the effective Lagrangians that are relevant to the radiative transition amplitudes of the pNGBs and light vector resonances below. We refer to Ref. [30] for details about the constructions of these Lagrangians. All of the Lagrangians are constructed in the framework of R χ T. In our scheme the $VP\gamma^*$ transition receives two types of contributions: the contact diagram and the resonance-exchange one, as shown in Fig. 2. The chiral effective Lagrangians with antisymmetric tensor formalism for the light vector resonances that are pertinent to these kinds of processes, are first written down in Ref. [57] and then completed in a more general setting in Ref. [58]. The focus of the previous two references is the $SU(3)$ case with the light pseudoscalar octet. We generalize the relevant discussions to the

$U(3)$ case in Ref. [30], so that we can study the processes involving η and η' states. The $U(3)$ operators with one vector resonance, one external source and one pNGB are given by

$$\begin{aligned}\mathcal{L}_{VJP} = & \frac{\tilde{c}_1}{M_V} \varepsilon_{\mu\nu\rho\sigma} \langle \{V^{\mu\nu}, \tilde{f}_+^{\rho\alpha}\} \nabla_\alpha \tilde{u}^\sigma \rangle + \frac{\tilde{c}_2}{M_V} \varepsilon_{\mu\nu\rho\sigma} \langle \{V^{\mu\alpha}, \tilde{f}_+^{\rho\sigma}\} \nabla_\alpha \tilde{u}^\nu \rangle + \frac{i\tilde{c}_3}{M_V} \varepsilon_{\mu\nu\rho\sigma} \langle \{V^{\mu\nu}, \tilde{f}_+^{\rho\sigma}\} \tilde{\chi}_- \rangle \\ & + \frac{i\tilde{c}_4}{M_V} \varepsilon_{\mu\nu\rho\sigma} \langle V^{\mu\nu} [\tilde{f}_-^{\rho\sigma}, \tilde{\chi}_+] \rangle + \frac{\tilde{c}_5}{M_V} \varepsilon_{\mu\nu\rho\sigma} \langle \{\nabla_\alpha V^{\mu\nu}, \tilde{f}_+^{\rho\alpha}\} \tilde{u}^\sigma \rangle + \frac{\tilde{c}_6}{M_V} \varepsilon_{\mu\nu\rho\sigma} \langle \{\nabla_\alpha V^{\mu\alpha}, \tilde{f}_+^{\rho\sigma}\} \tilde{u}^\nu \rangle \\ & + \frac{\tilde{c}_7}{M_V} \varepsilon_{\mu\nu\rho\sigma} \langle \{\nabla^\sigma V^{\mu\nu}, \tilde{f}_+^{\rho\alpha}\} \tilde{u}_\alpha \rangle - i\tilde{c}_8 M_V \sqrt{\frac{2}{3}} \varepsilon_{\mu\nu\rho\sigma} \langle V^{\mu\nu} \tilde{f}_+^{\rho\sigma} \rangle \ln(\det \tilde{u}),\end{aligned}\quad (19)$$

which are responsible for the contact diagram in Fig. 2. For the resonance-exchange diagram, the responsible effective Lagrangian reads

$$\begin{aligned}\mathcal{L}_{VVP} = & \tilde{d}_1 \varepsilon_{\mu\nu\rho\sigma} \langle \{V^{\mu\nu}, V^{\rho\alpha}\} \nabla_\alpha \tilde{u}^\sigma \rangle + i\tilde{d}_2 \varepsilon_{\mu\nu\rho\sigma} \langle \{V^{\mu\nu}, V^{\rho\sigma}\} \tilde{\chi}_- \rangle + \tilde{d}_3 \varepsilon_{\mu\nu\rho\sigma} \langle \{\nabla_\alpha V^{\mu\nu}, V^{\rho\alpha}\} \tilde{u}^\sigma \rangle \\ & + \tilde{d}_4 \varepsilon_{\mu\nu\rho\sigma} \langle \{\nabla^\sigma V^{\mu\nu}, V^{\rho\alpha}\} \tilde{u}_\alpha \rangle - i\tilde{d}_5 M_V^2 \sqrt{\frac{2}{3}} \varepsilon_{\mu\nu\rho\sigma} \langle V^{\mu\nu} V^{\rho\sigma} \rangle \ln(\det \tilde{u}).\end{aligned}\quad (20)$$

To impose the high energy constraints to the couplings can greatly reduce the number of free parameters in $R\chi T$ [26, 29, 48]. This procedure also renders the amplitudes calculated in $R\chi T$ consistent with the behavior dictated by QCD. We will follow this procedure in this work as well. Through matching the leading operator product expansion (OPE) of the VVP Green function with the result evaluated within $R\chi T$ and requiring the vector form factor to vanish in the high energy limit, we obtain the high energy constraints on resonance couplings [30]

$$\begin{aligned}4\tilde{c}_3 + \tilde{c}_1 &= 0, \\ \tilde{c}_1 - \tilde{c}_2 + \tilde{c}_5 &= 0, \\ \tilde{c}_5 - \tilde{c}_6 &= \frac{N_C}{64\pi^2} \frac{M_V}{\sqrt{2}F_V}, \\ \tilde{d}_1 + 8\tilde{d}_2 - \tilde{d}_3 &= \frac{F^2}{8F_V^2}, \\ \tilde{d}_3 &= -\frac{N_C}{64\pi^2} \frac{M_V^2}{F_V^2} \\ \tilde{c}_8 &= -\frac{\sqrt{2}M_0^2}{\sqrt{3}M_V^2} \tilde{c}_1.\end{aligned}\quad (21)$$

B. The transition amplitudes of $J/\psi \rightarrow P\gamma^*$

In accord with the covariant Lorentz structure, the general amplitude for the radiative decay $J/\psi(q) \rightarrow P(q-k)\gamma^*(k)$ takes the form

$$i\mathcal{M}_{\psi \rightarrow P\gamma^*} = ie \varepsilon_{\mu\nu\rho\sigma} \epsilon_\psi^\mu \epsilon_{\gamma^*}^\nu q^\rho k^\sigma G_{\psi \rightarrow P\gamma^*}(s), \quad (22)$$

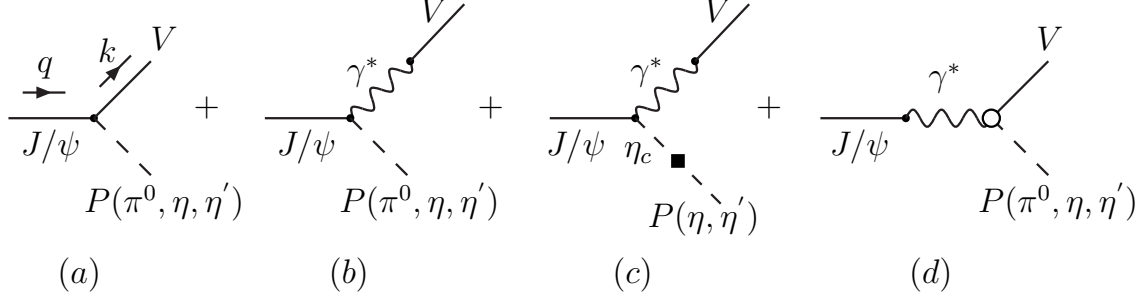


FIG. 1: Feynman diagrams for the processes $J/\psi \rightarrow VP$. The notations of the solid square in diagram (c) and the open circle in diagram (d) are explained in the text.

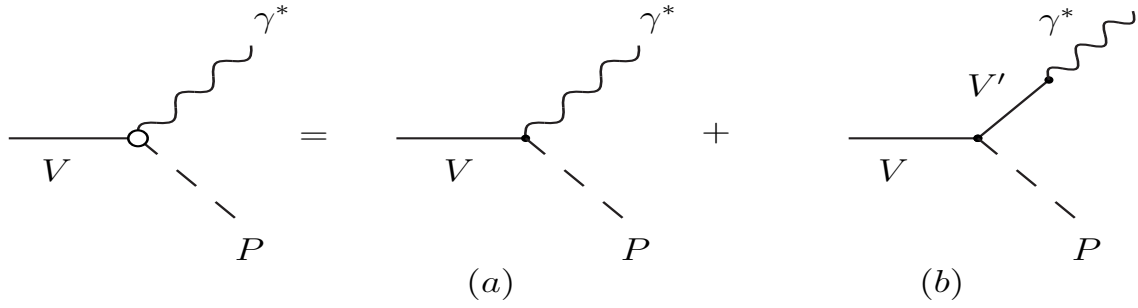


FIG. 2: Diagrams relevant to the $V \rightarrow P\gamma^*$ processes: (a) direct type and (b) indirect type.

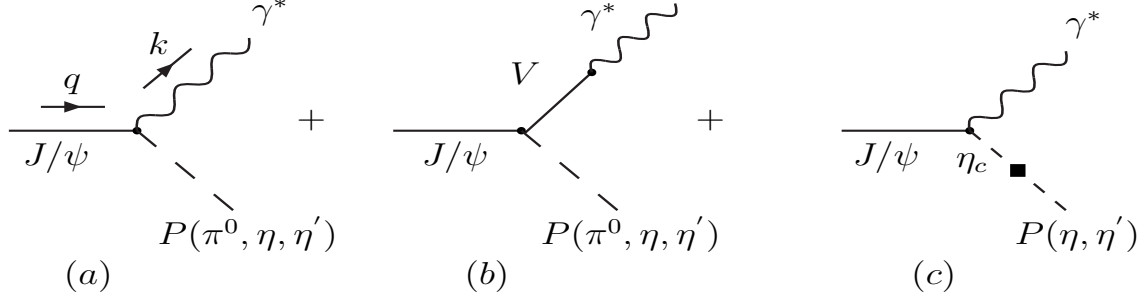
where q and k stand for the four momenta of J/ψ and γ^* respectively; $s = k^2$; ϵ_ψ and ϵ_{γ^*} are the polarization vectors; e is the electric charge of a positron. The relevant Feynman diagrams to the radiative decay $J/\psi \rightarrow P\gamma^*$ are displayed in Fig. 3. Using the previously introduced Lagrangian in Sec. II A, it is straightforward to calculate the contributions from the diagrams (a) and (b) in Fig. 3 to $G_{\psi \rightarrow P\gamma^*}(s)$. While for the diagram (c), we need to provide extra terms.

Based on the QCD axial anomaly and the PCAC hypothesis, the mixing angle of the $\eta(\eta') - \eta_c$ was evaluated in Ref. [7] and it was found that the mechanism from the diagram (c) in Fig. 3 dominates the $J/\psi \rightarrow \eta(\eta')\gamma$ decays. The contribution from this diagram to the $J/\psi \rightarrow \eta(\eta')\gamma$ amplitude can be generally written as

$$i\mathcal{M}_{\psi \rightarrow \eta(\eta')\gamma^*}^{mixing} = ie \varepsilon_{\mu\nu\rho\sigma} \epsilon_\psi^\mu \epsilon_{\gamma^*}^\nu q^\rho k^\sigma \lambda_{P\eta_c} g_{\psi\eta_c\gamma}(s) e^{i\delta_P}, \quad (23)$$

where the mixing strengths are obtained as $\lambda_{\eta\eta_c} = -4.6 \times 10^{-3}$, $\lambda_{\eta'\eta_c} = -1.2 \times 10^{-2}$ in Ref. [7]. δ_P , with $P = \eta, \eta'$, stand for the relative phases between diagram (c) and others, which are free parameters in this work and will be fitted later. The coupling strength $g_{\psi\eta_c\gamma}(s)$ is defined as

$$i\mathcal{M}_{\psi \rightarrow \eta_c\gamma^*} = ie \varepsilon_{\mu\nu\rho\sigma} \epsilon_\psi^\mu \epsilon_{\gamma^*}^\nu q^\rho k^\sigma g_{\psi\eta_c\gamma}(s), \quad (24)$$

FIG. 3: Feynman diagrams for the processes $J/\psi \rightarrow P\gamma^*$

and we can easily obtain

$$|g_{\psi\eta_c\gamma}(0)| = \left(\frac{24M_\psi^3\Gamma_{\psi\rightarrow\eta_c\gamma}}{\alpha(M_\psi^2 - m_{\eta_c}^2)^3} \right)^{\frac{1}{2}}. \quad (25)$$

Since we focus on the $J/\psi \rightarrow \eta_c\gamma^* \rightarrow \eta_c l^+ l^-$ process, the interval of the energy squared s is limited to a small region, comparing with the scale M_ψ^2 . This justifies us to use the spacelike form factor derived in Ref. [59]

$$g_{\psi\eta_c\gamma}(s) = g_{\psi\eta_c\gamma}(0)e^{\frac{s}{16\beta^2}}, \quad (26)$$

to the $s \sim 0$ timelike region, due to the continuity condition of the form factor at $s = 0$. In order not to interrupt the present discussions, the lengthy expressions of $G_{\psi\rightarrow P\gamma^*}(s)$ calculated from Fig. 3 are relegated in Appendix A.

In our convention, the decay widths of $J/\psi \rightarrow P\gamma$ are

$$\Gamma(\psi \rightarrow P\gamma) = \frac{1}{3}\alpha \left(\frac{M_\psi^2 - M_P^2}{2M_\psi} \right)^3 |G_{\psi\rightarrow P\gamma^*}(0)|^2, \quad (27)$$

and the decay widths of $J/\psi \rightarrow P\gamma^* \rightarrow Pl^+l^-$ are

$$\Gamma_{\psi\rightarrow Pl^+l^-} = \int_{4m_l^2}^{(M_\psi - m_P)^2} \frac{\alpha^2(2m_l^2 + s)}{72M_\psi^3\pi s^3} \sqrt{s(s - 4m_l^2)} [\lambda(s, M_\psi, m_P)]^3 |G_{\psi\rightarrow P\gamma^*}(s)|^2 ds, \quad (28)$$

where the leptons $l = e, \mu$, the pNGBs $P = \eta, \eta'$ and

$$\lambda(s, M_\psi, m_P) = \sqrt{[s - (M_\psi - m_P)^2][s - (M_\psi + m_P)^2]}. \quad (29)$$

C. Transition amplitudes of the $J/\psi \rightarrow VP$ processes

The general amplitude for the decay $J/\psi(q) \rightarrow V(k)P(q-k)$ in accord with the Lorentz structure can be written as

$$i\mathcal{M}_{\psi\rightarrow VP} = i\varepsilon_{\mu\nu\rho\sigma}\epsilon_\psi^\mu\epsilon_V^\nu q^\rho k^\sigma G_{\psi\rightarrow VP}, \quad (30)$$

and the relevant Feynman diagrams are displayed in Fig. 1. The diagram (a) in Fig. 1 represents the strong interaction part, which can be evaluated with the Lagrangian in Eq. (15). The remaining diagrams receive EM contributions, which can be evaluated with the Lagrangians in Eqs. (14)(16)(17)(19)(20) and the amplitude in Eq. (23).

For the diagram (d) in Fig. 1, we need the amplitudes of $V(k)P(q-k)\gamma^*(q)$, which are depicted in Fig. 2 and can be written as

$$i\mathcal{M}_{VP\gamma^*} = -ie\varepsilon_{\mu\nu\rho\sigma}\epsilon_V^\mu\epsilon_{\gamma^*}^\nu q^\rho k^\sigma F_{VP\gamma^*}(s=q^2). \quad (31)$$

The form factors $F_{VP\gamma^*}(s)$ are calculated within the framework of R χ T in Ref. [30] and we simply give the results in Appendix B for completeness. In this convention, the contribution from the diagram (d) in Fig. 1 to the $G_{\psi\rightarrow VP}$ is found to be $\frac{8\sqrt{2}\pi\alpha}{3}\frac{f_\psi}{M_\psi}F_{VP\gamma^*}(s=M_\psi^2)$.

The full expressions of $G_{\psi\rightarrow VP}$ from Fig. 1 are relegated in Appendix C. The decay widths of $J/\psi \rightarrow VP$ are given by

$$\Gamma(\psi \rightarrow VP) = \frac{1}{96\pi M_\psi^3} \left\{ [M_\psi^2 - (M_V - m_P)^2] [M_\psi^2 - (M_V + m_P)^2] \right\}^{\frac{3}{2}} |G_{\psi\rightarrow VP}|^2. \quad (32)$$

III. PHENOMENOLOGY DISCUSSION

The experimental data that we consider in this work include the decay widths of $J/\psi \rightarrow P\gamma$ and $J/\psi \rightarrow VP$ [34], with $P = \pi, K, \eta, \eta'$ and $V = \rho, K^*, \omega, \phi$, and the recently measured Dalitz decay widths of $J/\psi \rightarrow Pe^+e^-$ and the form factor $|F_{\psi\eta'}(s)|^2 = \left| \frac{G_{\psi\rightarrow\eta'\gamma^*}(s)}{G_{\psi\rightarrow\eta'\gamma^*}(0)} \right|^2$ [33].¹ Also we take into account all the radiative decay processes considered in our previous paper with only light hadron states [30]: $P \rightarrow V\gamma$, $V \rightarrow P\gamma$, $P \rightarrow \gamma\gamma$, $P \rightarrow \gamma l^+ l^-$, $V \rightarrow Pl^+ l^-$, as well as the form factors of $\eta \rightarrow \gamma\gamma^*$, $\eta' \rightarrow \gamma\gamma^*$, $\phi \rightarrow \eta\gamma^*$. Below we will make a global fit by taking the two types of data together, i.e. these with the J/ψ and those without the J/ψ .

For the resonance operators c_i and d_j in Eqs. (19) and (20), we impose the high energy constraints presented in Eq. (21), in such a way it reduces six combinations of unknown parameters and is quite helpful to stabilize the fit. In addition, it makes the asymptotic behaviors of the relevant amplitudes consistent with QCD in the large N_C and chiral limits. The \tilde{c}_4 term in Eq. (19), which contributes exclusively to the vertex $K^{*\pm}K^\pm\gamma$, is the focus of Ref. [31], and $\tilde{c}_4 = -0.0023$

¹ In Ref. [33], the peaking backgrounds arising from $J/\psi \rightarrow PV \rightarrow Pe^+e^-$, with $V = \rho^0, \omega, \phi$, are subtracted. We acknowledge Xin-Kun Chu for patient explanations on this issue. In accord with the experimental measurements, we do not consider the contribution from the diagram (b) in Fig. 3 when fitting the data from Ref. [33]. To be consistent, the theoretical predictions for the decay widths of $J/\psi \rightarrow P\mu^+\mu^-$ given in Table IV are obtained by excluding the diagram (b) in Fig. 3.

is determined there. In Ref. [30], a very strong linear correlation between \tilde{d}_2 and \tilde{d}_5 is observed: $\tilde{d}_5 = 4.4\tilde{d}_2 - 0.06$. We will take this value of \tilde{c}_4 and use the linear correlation between \tilde{d}_2 and \tilde{d}_5 in our current study, and we point out that if the values of \tilde{c}_4 , \tilde{d}_2 and \tilde{d}_5 are fitted, the results turn out to be very close to these constraints. For β in Eq. (26), we will take the value $\beta = 580 \pm 19$ MeV [60]. Our fitting quality is not sensitive to the value of β if β is above 500 MeV. The reason behind is that for the $J/\psi \rightarrow \eta(\eta')l^+l^-$ decays the dominant contributions come from the region with small values of s , due to the kinematic factors in Eq. (28). In addition, the experiment data for the $J/\psi \rightarrow \eta'\gamma^*$ form factors have large errors, as shown in Fig. 4.

Before stepping into the detail of the fits, we point out that with the theoretical setups in Sect. II there are always large discrepancies between our theoretical output and the experimental measurement for the isospin-violated channel $J/\psi \rightarrow \omega\pi^0$. Similarly large discrepancies have also been found between the conventional VMD approach and the experimental data of $\omega \rightarrow \pi^0\gamma^*$ form factors [61, 62], and one possible solution is to include more excited resonances [31, 63]. Therefore in order to reasonably describe the $J/\psi \rightarrow \omega\pi^0$ decay, we simply introduce another excited vector resonance ρ' in this channel. To be more specific, we introduce the term $r_1 M_\omega D_{\rho'}(s)$ to the form factor $F_{\omega\pi\gamma^*}(s)$ in Eq. (31) and the definition of the propagator $D_{\rho'}(s)$ is given in Eq. (A4). The parameter r_1 will be fitted. The mass and width of ρ' will be fixed at $M_{\rho'} = 1600$ MeV and $\Gamma_{\rho'} = 500$ MeV, respectively. We point out that a sizable variation of $M_{\rho'}$ and $\Gamma_{\rho'}$ barely affects the fitting results.

With all of the previous setups, it is ready to present our fit results. The final values for the fitted parameters are given in Table I. For the various decay widths, we summarize the experiment data and the results from our theoretical outputs in Table II for the J/ψ decay processes and in Table III for the light-hadron decays. The resulting plots for the form factors of $J/\psi\eta'\gamma^*$, $\eta\gamma\gamma^*$, $\eta'\gamma\gamma^*$ and $\phi\eta\gamma^*$ together with the corresponding experimental data are given in Figs. 4, 5, 6 and 7, respectively. The error bands shown in the plots and the errors of the physical quantities in the following tables correspond to the statistical uncertainties at one standard deviation [64]: $n_\sigma = (\chi^2 - \chi_0^2)/\sqrt{2\chi_0^2}$, with χ_0^2 the minimum χ^2 obtained in the fit and n_σ the number of standard deviations.

Some remarks for the fitting results are in order. We comment them one by one as follows.

1. The $\eta - \eta'$ mixing parameters. In the $U(3)$ χ PT, F_8 can be fixed through the ratio of F_K/F_π at the next-to-next-to-leading order within the triple expansion scheme, i.e. a simultaneous expansion on the momentum, quark mass and $1/N_C$. This approach leads to the prediction

	Fit	Fit in Ref. [30]
F_8	$(1.45 \pm 0.04)F_\pi$	$(1.37 \pm 0.07)F_\pi$
F_0	$(1.28 \pm 0.06)F_\pi$	$(1.19 \pm 0.18)F_\pi$
θ_8	$(-26.7 \pm 1.8)^\circ$	$(-21.1 \pm 6.0)^\circ$
θ_0	$(-11.0 \pm 1.0)^\circ$	$(-2.5 \pm 8.2)^\circ$
F_V	134.9 ± 3.2	136.6 ± 3.5
\tilde{c}_3	0.0029 ± 0.0006	0.0109 ± 0.0161
\tilde{d}_2	0.081 ± 0.006	0.086 ± 0.085
h_1	$(-2.36 \pm 0.13) \times 10^{-5}$	-
h_2	$(-4.73 \pm 1.26) \times 10^{-5}$	-
h_3	$(3.85 \pm 0.45) \times 10^{-6}$	-
g_1	$(-2.92 \pm 0.17) \times 10^{-5}$	-
g_2	$(5.93 \pm 1.04) \times 10^{-4}$	-
r_1	0.44 ± 0.10	-
δ_η	$(39 \pm 44)^\circ$	-
$\delta_{\eta'}$	$(115 \pm 13)^\circ$	-
$\frac{\chi^2}{d.o.f}$	$\frac{96.0}{106-15} = 1.06$	$\frac{64.0}{70-8} = 1.03$
F_q	$(1.15 \pm 0.04)F_\pi$	-
F_s	$(1.56 \pm 0.06)F_\pi$	-
ϕ_q	$(34.5 \pm 1.8)^\circ$	-
ϕ_s	$(36.0 \pm 1.4)^\circ$	-

TABLE I: The parameters result from the fit. For comparison, we provide the results of Ref. [30] which are obtained by only fitting the light hadrons radiative decay processes.

$F_8 = 1.34F_\pi$ [53]. While for F_0 , according to the results from our previous work with only light hadrons [30], its error bar is much larger than that of F_8 . After including the J/ψ data, we find that the error bar of F_0 is now compatible with the one for F_8 , indicating the sensitivity of this parameter in J/ψ decays. F_0 was determined in the process $P \rightarrow \gamma\gamma$ at next-to-leading order by ignoring the chiral symmetry breaking operators in Refs. [41, 42], which led to $F_0 = 1.25F_\pi$. As one can see the numbers in Table I, our result for F_8 is slightly larger than the χ PT prediction, and our F_0 agrees with the χ PT prediction. About the mixing angles, our present determinations for θ_8 and θ_0 are somewhat more negative than those in literature, see Table 1 of Ref. [37]. Comparing with our previous determinations in Ref. [30] with only light hadron data, the present values for the two angles also become more negative, see the last two columns in Table I. This tells us that the J/ψ data prefer somewhat more negative mixing angles. Nevertheless, when taking into account the errors of these two parameters as shown in Table I, the results of θ_8 and θ_0 in this analysis are still comparable with previous studies. It is clear that the present error bands of θ_0 and θ_8 are

	Exp	Fit
$\psi \rightarrow \rho^0 \pi^0$	5.3 ± 0.7	5.6 ± 0.7
$\psi \rightarrow \rho \pi$	16.9 ± 1.5	16.4 ± 1.9
$\psi \rightarrow \rho^0 \eta$	0.193 ± 0.023	0.202 ± 0.047
$\psi \rightarrow \rho^0 \eta'$	0.105 ± 0.018	0.110 ± 0.035
$\psi \rightarrow \omega \pi^0$	0.45 ± 0.05	0.45 ± 0.12
$\psi \rightarrow \omega \eta$	1.74 ± 0.20	1.74 ± 0.25
$\psi \rightarrow \omega \eta'$	0.182 ± 0.021	0.184 ± 0.040
$\psi \rightarrow \phi \eta$	0.75 ± 0.08	0.82 ± 0.11
$\psi \rightarrow \phi \eta'$	0.40 ± 0.07	0.38 ± 0.13
$\psi \rightarrow K^{*+} K^- + \text{c.c.}$	5.12 ± 0.30	4.79 ± 0.51
$\psi \rightarrow K^{*0} \bar{K}^0 + \text{c.c.}$	4.39 ± 0.31	4.43 ± 0.38
$\psi \rightarrow \pi^0 \gamma$	0.0349 ± 0.0032	0.0303 ± 0.0086
$\psi \rightarrow \eta \gamma$	1.104 ± 0.034	1.101 ± 0.079
$\psi \rightarrow \eta' \gamma$	5.16 ± 0.15	5.22 ± 0.15
$\psi \rightarrow \pi^0 e^+ e^-$	$(0.0756 \pm 0.0141) \times 10^{-2}$	$(0.1191 \pm 0.0138) \times 10^{-2}$
$\psi \rightarrow \eta e^+ e^-$	$(1.16 \pm 0.09) \times 10^{-2}$	$(1.16 \pm 0.08) \times 10^{-2}$
$\psi \rightarrow \eta' e^+ e^-$	$(5.81 \pm 0.35) \times 10^{-2}$	$(5.76 \pm 0.16) \times 10^{-2}$

TABLE II: Experimental and theoretical values of the branching fractions ($\times 10^{-3}$) of various processes: $J/\psi \rightarrow VP$, $J/\psi \rightarrow P\gamma$, and $J/\psi \rightarrow Pe^+e^-$. The experimental data are taken from [33, 34]. The error bands of the theoretical outputs are calculated by using the parameter configurations in Table I.

much smaller than the values in Ref. [30], which highlights the relevance of the J/ψ data in the determination of the η - η' mixing parameters.

For the mixing parameters in the quark-flavor basis defined in Eq. (7), the theoretical prediction for the difference between the angles ϕ_q and ϕ_s should be very small, since their difference is caused by the OZI-rule violating terms. In this work, we further confirm this prediction and the difference between ϕ_q and ϕ_s is indeed found to be tiny. Our results, $\phi_q = (34.5 \pm 1.8)^\circ$ and $\phi_s = (36.0 \pm 1.4)^\circ$, are in qualitative agreement with these earlier studies in Refs. [3, 37], which give the result around 40° . Our analysis prefers slightly smaller magnitudes of ϕ_q and ϕ_s .

2. The \tilde{c}_3 and \tilde{d}_2 parameters were determined with huge error bars in our previous study without the J/ψ data [30]. We see that the present results are compatible with those in [30], but

	Exp	Fit
$\Gamma_{\omega \rightarrow \pi \gamma}$	757 ± 28	750 ± 33
$\Gamma_{\rho^0 \rightarrow \pi^0 \gamma}$	89.6 ± 12.6	78.0 ± 3.4
$\Gamma_{K^{*0} \rightarrow K^0 \gamma}$	116 ± 12	116 ± 5
$\Gamma_{\omega \rightarrow \eta \gamma}$	3.91 ± 0.38	5.16 ± 0.41
$\Gamma_{\rho^0 \rightarrow \eta \gamma}$	44.8 ± 3.5	42.6 ± 3.5
$\Gamma_{\phi \rightarrow \eta \gamma}$	55.6 ± 1.6	55.4 ± 3.7
$\Gamma_{\phi \rightarrow \eta' \gamma}$	0.265 ± 0.012	0.265 ± 0.027
$\Gamma_{\eta' \rightarrow \omega \gamma}$	6.2 ± 1.1	6.2 ± 0.4
$\Gamma_{\eta \rightarrow \gamma \gamma}$	0.510 ± 0.026	0.463 ± 0.038
$\Gamma_{\eta' \rightarrow \gamma \gamma}$	4.30 ± 0.15	4.13 ± 0.26
$\Gamma_{\eta \rightarrow \gamma e^- e^+}$	$(8.8 \pm 1.6) \times 10^{-3}$	$(7.7 \pm 0.6) \times 10^{-3}$
$\Gamma_{\eta \rightarrow \gamma \mu^- \mu^+}$	$(0.40 \pm 0.08) \times 10^{-3}$	$(0.36 \pm 0.03) \times 10^{-3}$
$\Gamma_{\eta' \rightarrow \gamma \mu^- \mu^+}$	$(2.1 \pm 0.7) \times 10^{-2}$	$(1.6 \pm 0.1) \times 10^{-2}$
$\Gamma_{\omega \rightarrow \pi e^- e^+}$	6.54 ± 0.83	6.81 ± 0.30
$\Gamma_{\omega \rightarrow \pi \mu^- \mu^+}$	0.82 ± 0.21	0.67 ± 0.03
$\Gamma_{\phi \rightarrow \eta e^- e^+}$	0.490 ± 0.048	0.464 ± 0.031

TABLE III: Experimental and theoretical values of the decay widths of various processes: $P \rightarrow V\gamma$, $V \rightarrow P\gamma$, $P \rightarrow \gamma\gamma$, $P \rightarrow \gamma l^+ l^-$, $V \rightarrow Pl^+ l^-$. The experimental data are taken from [34]. All of the values are given in units of KeV. The error bands of the theoretical outputs are calculated by using the parameter configurations in Table I.

have smaller error bars now. The magnitude of \tilde{c}_3 is of order 10^{-3} now, which is consistent with the magnitudes of \tilde{c}_4 and \tilde{c}_6 determined in Ref. [31].

3. The $J/\psi \rightarrow Pl^+ l^-$ process. In Ref. [13], the form factor of $J/\psi \rightarrow P\gamma^*$ is parameterized by using the simple pole approximation in the VMD framework as

$$F_{\psi P}(s) \equiv \frac{G_{\psi \rightarrow P\gamma^*}(s)}{G_{\psi \rightarrow P\gamma^*}(0)} = \frac{1}{1 - s/\Lambda^2}, \quad (33)$$

with Λ chosen to be the mass of ψ' . We plot the integrand of Eq. (28), namely the differential decay widths for $J/\psi \rightarrow Pl^+ l^-$ in Fig. 8, from which it is not difficult to observe that the $J/\psi \rightarrow Pl^+ l^-$ decay width is dominated by the small s region, purely due to the kinematic factors. Therefore the s/Λ^2 term in Eq. (33) cannot give large effect. This also explains that different values of β in the form factor $e^{\frac{s}{16\beta^2}}$ in Eq. (26) make little difference. Thus for the $J/\psi \rightarrow Pl^+ l^-$ decay rate, the overwhelmingly dominant part is from the structure

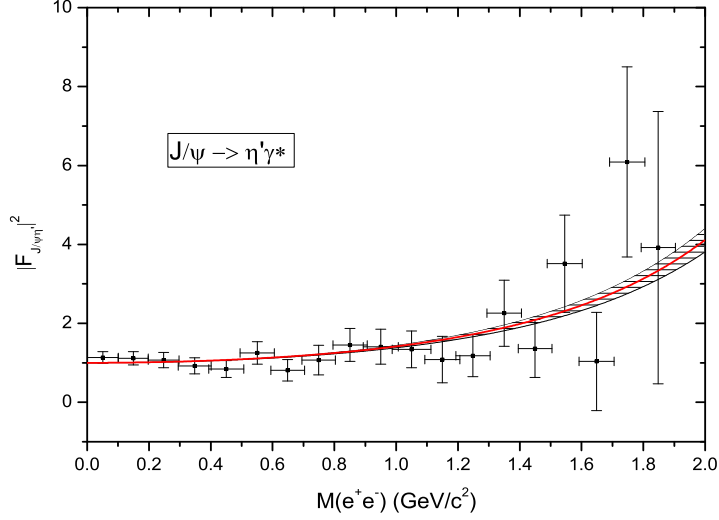


FIG. 4: (Color online). The form factors of $J/\psi \rightarrow \eta'\gamma^*$. The red solid line corresponds to the result with the central values of the parameters in Table I and the shaded areas stand for the error bands. The experimental data are taken from [33].

independent factor $F_{\psi P}(s) = 1$ and any model-dependent hadronic corrections to $F_{\psi P}(s) = 1$ will only slightly affect the total decay rate.

At a first glance, the theoretical model we propose to study the $J/\psi \rightarrow Pl^+l^-$ decay, which is schematically depicted in Fig. 3, is clearly different from the VMD model in Eq. (33), since we do not explicitly include the effects of ψ' in Fig. 3. Nevertheless, as discussed just before, what matters to the decay rate of $J/\psi \rightarrow Pl^+l^-$ is the very low energy region of the integrand in Eq. (28), where the propagator of the ψ' from the VMD approach in Eq. (33) reduces to a constant. Essentially, the diagrams (a) and (c) in Fig. 3 give constant terms in the low energy region. While the diagram (b) has to be subtracted in order to be consistent with experimental setup, as the contributions from the light vector resonances have been removed in the final results from experimental analyses [33]. Therefore we can conclude that our model in Fig. 3 is qualitatively similar as the commonly used VMD model in Eq. (33) when focusing on the $J/\psi \rightarrow Pl^+l^-$ decay width. The theoretical outputs and the experimental data of the $J/\psi \rightarrow Pl^+l^-$ processes are summarized in Table IV.

Both our theoretical outputs and the VMD predictions for the $J/\psi \rightarrow \eta(\eta')e^+e^-$ processes agree with the data, as shown in Table IV. While for the $J/\psi \rightarrow \pi^0e^+e^-$ process, none of the results from the two approaches are compatible with the experimental data. Notice that for

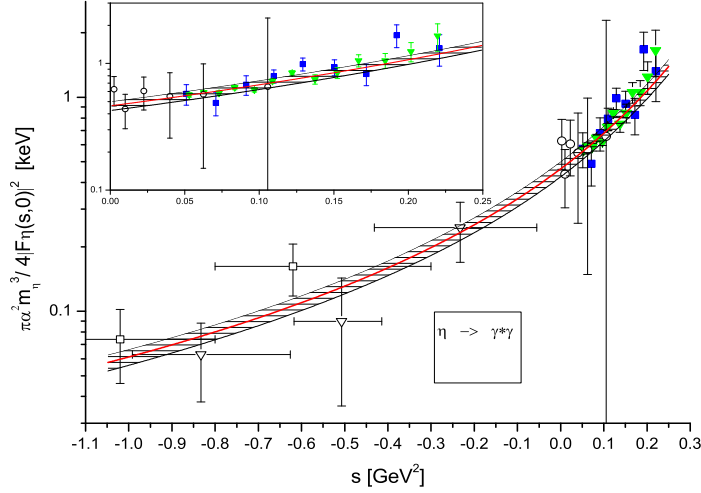


FIG. 5: (Color online). The form factors of $\eta \rightarrow \gamma^* \gamma$. The red solid line corresponds to the result with the central values of the parameters in Table I and the shaded areas stand for the error bands. The references of different experimental data are: solid squares [67, 68], open squares [69], open circles [70], solid triangles [71] and open triangles [72]. The framed figure is the close-up of the plot in the region of $s > 0$.

the experimental analyses of the $J/\psi \rightarrow P e^+ e^-$ decays in Ref. [33], the peaking backgrounds from the intermediate processes like $J/\psi \rightarrow \rho^0 P, \omega P$ and ϕP , with ρ^0, ω and ϕ decaying into $e^+ e^-$, have been subtracted. From the world average results in Ref. [34], we know the branching ratios $B_{J/\psi \rightarrow \rho^0 \pi^0} = (5.6 \pm 0.7) \times 10^{-3}$ and $B_{\rho^0 \rightarrow e^+ e^-} = (4.72 \pm 0.05) \times 10^{-5}$, so that $B_{J/\psi \rightarrow \rho^0 \pi^0} \times B_{\rho^0 \rightarrow e^+ e^-} = (2.64 \pm 0.36) \times 10^{-7}$, which is about 1/3 of the branching ratio $B_{J/\psi \rightarrow \pi^0 e^+ e^-}$ given in Ref. [33]. This rough estimate tells us that the contributions from the intermediate processes with light hadrons can be important and this conclusion is in accord with the dispersive analyses in Ref. [65]. Our simple estimate also confirms the findings in Refs. [12, 66], where the dominance of $J/\psi \rightarrow \pi^0 \rho^0 \rightarrow \pi^0 \gamma$ in the $J/\psi \rightarrow \pi^0 \gamma$ decay is evident. In our theoretical scheme, we find large destructive interference between the intermediate- ρ^0 's contribution and other contributions in the $J/\psi \rightarrow \pi^0 \gamma$ and the $J/\psi \rightarrow \pi^0 l^+ l^-$ processes, so that neglecting the intermediate- ρ^0 's contribution leads to a larger value of the branching ratio of $J/\psi \rightarrow \pi^0 e^+ e^-$.

Therefore we urge the experimental colleagues to take more serious analyses of the light vector contributions in the $J/\psi \rightarrow \pi^0 e^+ e^-$ decays in order to clarify its decay mechanism. We find that the contributions from the intermediate light vectors are tiny in the $J/\psi \rightarrow \eta(\eta') \gamma$ and

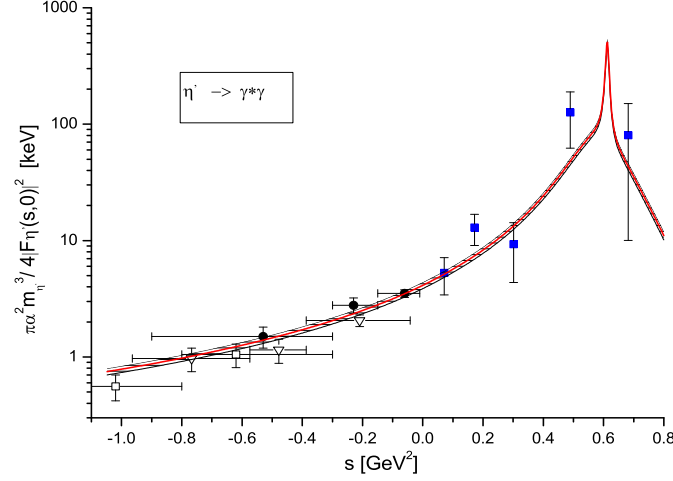


FIG. 6: The form factors of $\eta' \rightarrow \gamma^* \gamma$. The red solid line corresponds to the result with the central values of the parameters in Table I and the shaded areas stand for the error bands. The references of different experimental data are: solid squares [67, 68], open squares [69], open triangles [72], solid circles [73].

$J/\psi \rightarrow \eta(\eta') l^+ l^-$ processes.

In addition, we provide the predictions for the $J/\psi \rightarrow P \mu^+ \mu^-$ decays in Table IV together with the results from Ref. [13]. We hope our results can provide to the experimental colleagues some references for future measurements on these channels.

	Exp. data	this work	VMD prediction [13]
$\psi \rightarrow \pi^0 e^+ e^-$	0.0756 ± 0.0141	0.1191 ± 0.0138	$0.0389^{+0.0037}_{-0.0033}$
$\psi \rightarrow \eta e^+ e^-$	1.16 ± 0.09	1.16 ± 0.08	1.21 ± 0.04
$\psi \rightarrow \eta' e^+ e^-$	5.81 ± 0.35	5.76 ± 0.16	5.66 ± 0.16
$\psi \rightarrow \pi^0 \mu^+ \mu^-$	-	0.0280 ± 0.0032	$0.0101^{+0.0010}_{-0.0009}$
$\psi \rightarrow \eta \mu^+ \mu^-$	-	0.32 ± 0.02	0.30 ± 0.01
$\psi \rightarrow \eta' \mu^+ \mu^-$	-	1.46 ± 0.04	1.31 ± 0.04

TABLE IV: Branching ratios ($\times 10^{-5}$) for $J/\psi \rightarrow P l^+ l^-$, where $P = \pi^0, \eta, \eta'$, and $l = e, \mu$.

4. $\eta(\eta') - \eta_c$ mixing. For the $J/\psi \rightarrow \eta(\eta') \gamma^{(*)}$ processes, if we do not include the mechanism raised in Ref. [7], i.e. the diagram (c) in Fig. 3, there is no way for us to simultaneously describe the $J/\psi \rightarrow \eta(\eta') \gamma^{(*)}$ processes together with other types of data. Therefore we

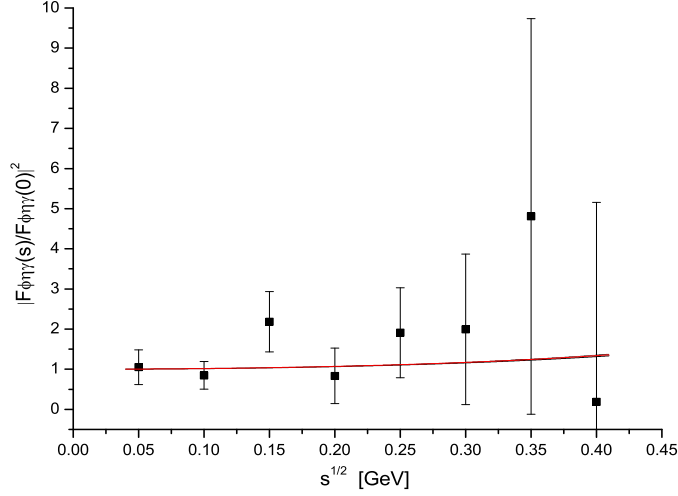


FIG. 7: The form factors of $\phi \rightarrow \eta\gamma^*$ [70]. The red solid line corresponds to the result with the central values of the parameters in Table I and the shaded areas stand for the error bands.

confirm the importance of the $\eta(\eta')\text{-}\eta_c$ mixing in $J/\psi \rightarrow \eta(\eta')\gamma^{(*)}$ as advocated in Ref. [7, 12]. In Table V, we quantitatively show the contributions from the diagram (c) in Fig. 3 to the total decay widths of $J/\psi \rightarrow \eta(\eta')\gamma$ and $J/\psi \rightarrow \eta(\eta')e^+e^-$.

	Exp. data	η_c mixing in this work	η_c mixing in Ref. [12]
$\psi \rightarrow \eta\gamma$	1.104 ± 0.034	0.823	0.61
$\psi \rightarrow \eta'\gamma$	5.16 ± 0.15	4.56	3.5
$\psi \rightarrow \eta e^+e^-$	$(1.16 \pm 0.09) \times 10^{-2}$	0.95×10^{-2}	-
$\psi \rightarrow \eta' e^+e^-$	$(5.81 \pm 0.35) \times 10^{-2}$	5.07×10^{-2}	-

TABLE V: Branching ratios ($\times 10^{-3}$) for $J/\psi \rightarrow \eta(\eta')\gamma$, and $J/\psi \rightarrow \eta(\eta')e^+e^-$ caused by the $\eta(\eta') - \eta_c$ mixing.

5. The roles of the EM and strong transitions in the $J/\psi \rightarrow VP$ decays. In order to discuss the interplay roles of the EM and strong interactions in the $J/\psi \rightarrow VP$ processes, we show the modulus of the form factors G_{VP} defined in Eq. (30) in Table VI. In the left side of this table we show the contributions from strong interactions to the isospin conserved channels and in the right side we show the EM contributions to the isospin violated channels. It is clear that the strong interactions play the dominant roles in the isospin conserved decay channels and the EM interactions dominate the isospin violated channels. Furthermore, for the isospin

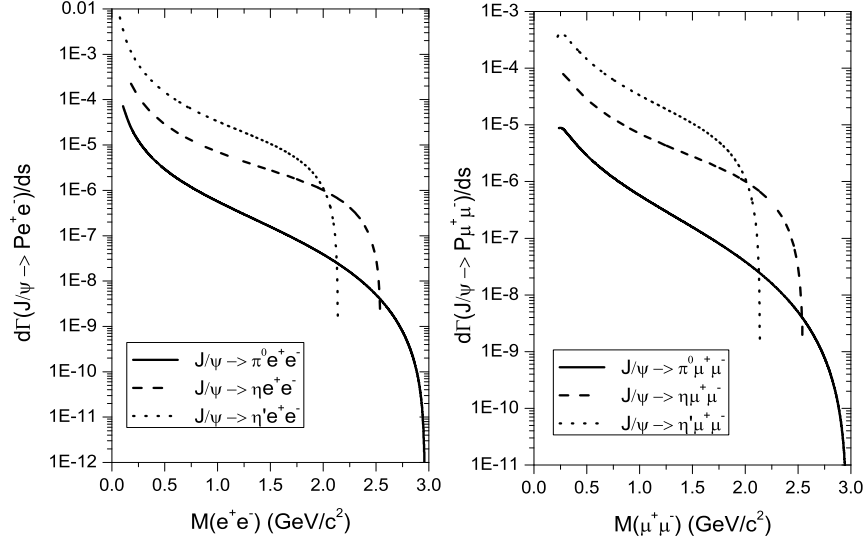


FIG. 8: The differential decay widths of $J/\psi \rightarrow Pl^+l^-$ processes, where the solid line is for $J/\psi \rightarrow \pi^0 l^+l^-$, the dashed line for $J/\psi \rightarrow \eta l^+l^-$, and the dotted line for $J/\psi \rightarrow \eta' l^+l^-$. The left panel is for the lepton pair e^+e^- and the right panel for the lepton pair $\mu^+\mu^-$.

conserved cases we have explicitly checked that there are no significant contributions from the EM transitions, with the exception of the $J/\psi \rightarrow \phi\eta'$ channel. We find that there is a large destructive interference between the strong and EM interactions in this process. Generally speaking, our findings in $J/\psi \rightarrow VP$ decays are consistent with a general expectation and our numbers are in qualitative agreement with those in Ref. [18].

Isospin conserved cases	Exp. data	Strong interaction	Isospin violated cases	Exp. data	EM interaction
$ G_{\psi \rightarrow \rho^0 \pi^0} $	2.541 ± 0.154	2.933 ± 0.144	$ G_{\psi \rightarrow \rho^0 \eta} $	0.498 ± 0.029	0.510 ± 0.056
$ G_{\psi \rightarrow \rho \pi} $	4.415 ± 0.192	5.080 ± 0.250	$ G_{\psi \rightarrow \rho^0 \eta'} $	0.418 ± 0.034	0.429 ± 0.063
$ G_{\psi \rightarrow \omega \eta} $	1.499 ± 0.084	1.628 ± 0.097	$ G_{\psi \rightarrow \omega \pi^0} $	0.722 ± 0.039	0.722 ± 0.091
$ G_{\psi \rightarrow \omega \eta'} $	0.552 ± 0.031	0.659 ± 0.059			
$ G_{\psi \rightarrow \phi \eta} $	1.069 ± 0.056	1.346 ± 0.066			
$ G_{\psi \rightarrow \phi \eta'} $	0.910 ± 0.076	1.178 ± 0.126			
$ G_{\psi \rightarrow K^{*+} K^-} $	1.860 ± 0.054	2.473 ± 0.089			
$ G_{\psi \rightarrow K^{*0} \bar{K}^0} $	1.726 ± 0.060	2.468 ± 0.082			

TABLE VI: The modulus of form factor $|G_{\psi \rightarrow VP}|$ in units of 10^{-6}MeV^{-1} contributed by the strong transitions to the isospin conserved channels, and by the EM transitions to the isospin violated channels. The error bands from this table are calculated by using the same parameter configurations as in Table I.

IV. CONCLUSIONS

We use the effective Lagrangian approach to simultaneously study the decays of $J/\psi \rightarrow VP$, $J/\psi \rightarrow P\gamma$, $J/\psi \rightarrow Pl^+l^-$ together with the light meson radiative processes, such as $VP\gamma^{(*)}$, $P\gamma\gamma^{(*)}$. We take the building blocks involving external sources, light pseudoscalar mesons and vector resonances from the chiral effective field theory to construct the effective Lagrangian for the J/ψ decays. The $SU(3)$ -flavor symmetry breaking effects and the OZI rules are systematically and concisely implemented in this approach. For the processes with only light hadrons, we follow closely our previous work in Ref. [30] and use the resonance chiral theory to build the relevant Lagrangians. Two-mixing-angle scheme from the general discussion in $U(3)$ chiral perturbation theory is employed to describe the η - η' mixing in various processes involving η or η' . Comparing with our previous results by taking only the light hadron data in the analyses, we update the values for the mixing parameters by including the relevant J/ψ decays in this work. It turns out that the present determination prefers more negative values for the two mixing angles θ_0 and θ_8 from the octet-singlet basis, or smaller values for the ϕ_q and ϕ_s from the quark-flavor basis. Since we make a global fit for the J/ψ and the light hadron data in this work, smaller error bars result for some of the couplings in Table I, especially for \tilde{c}_3 and θ_0 . This clearly indicates the relevance of the J/ψ data for the determinations of the couplings involving only light hadrons and the η - η' mixing parameters.

In a short summary, we have found a proper theoretical framework that can be used to systematically and successfully describe the $J/\psi \rightarrow VP$, $P\gamma^{(*)}$ and the light meson radiative decays. Another interesting and relevant subjects along this research line is to take the $\psi(2S) \rightarrow VP$ and $\psi(2S) \rightarrow P\gamma$ into account, so that the famous $\rho\pi$ puzzle in charmonium decays could be addressed. Nevertheless, a straightforward generalization of the decay mechanisms from J/ψ to $\psi(2S)$ might be problematic, as recently discussed in Ref. [74]. Moreover, due to the fact that the low statistics for the $\psi(2S)$ data can not be compared to the precise ones of the J/ψ and light hadrons, it is not so clear whether it is justified to make a global fit by including the $\psi(2S)$ data as the ones considered in this work. Therefore we think it is worthy starting an independent project to study the $\psi(2S)$ decays, specially to address the long standing $\rho\pi$ puzzle, which is under preparation.

Acknowledgments

We acknowledge Xin-Kun Chu, Jian-Ping Dai, and Rong-Gang Ping from BESIII collaboration for helpful discussions on the experimental analyses. This work is supported in part by the National Natural Science Foundation of China under Grants No. 11105038, No. 11035006, No. 11121092, and No. 11261130311 (CRC110 by DFG and NSFC), the Chinese Academy of Sciences under Project No. KJCX2-EW-N01, and the Ministry of Science and Technology of China (2009CB825200). Z.H.G. acknowledges the grants from the Education Department of Hebei Province under Contract No. YQ2014034, the grants from the Department of Human Resources and Social Security of Hebei Province with contract No. C201400323, and the Doctor Foundation of Hebei Normal University under Contract No. L2010B04.

Appendix A: The form factors of $J/\psi \rightarrow P\gamma^*$

For latter convenience, we define several a_i factors as follows

$$\begin{aligned} a_1 &= \frac{F}{\cos(\theta_0 - \theta_8)} \left(\frac{1}{\sqrt{6}} \frac{\cos \theta_0}{F_8} - \frac{1}{\sqrt{3}} \frac{\sin \theta_8}{F_0} \right), \\ a_2 &= \frac{F}{\cos(\theta_0 - \theta_8)} \left(\frac{1}{\sqrt{6}} \frac{\sin \theta_0}{F_8} + \frac{1}{\sqrt{3}} \frac{\cos \theta_8}{F_0} \right), \\ a_3 &= \frac{F}{\cos(\theta_0 - \theta_8)} \left(-\frac{2}{\sqrt{6}} \frac{\cos \theta_0}{F_8} - \frac{1}{\sqrt{3}} \frac{\sin \theta_8}{F_0} \right), \\ a_4 &= \frac{F}{\cos(\theta_0 - \theta_8)} \left(-\frac{2}{\sqrt{6}} \frac{\sin \theta_0}{F_8} + \frac{1}{\sqrt{3}} \frac{\cos \theta_8}{F_0} \right). \end{aligned}$$

The explicit expressions for the form factors of the $J/\psi \rightarrow P\gamma^*$ defined in Eq. (22) are given below:

$$G_{\psi \rightarrow \pi^0 \gamma^*}(s) = -\frac{4g_1}{F_\pi} - \frac{16g_2}{F_\pi M_\psi^2} m_\pi^2 + 2\sqrt{2}h_1 M_\psi \frac{F_V}{F_\pi} D_\rho(s) + 8\sqrt{2}h_2 \frac{m_\pi^2}{M_\psi} \frac{F_V}{F_\pi} D_\rho(s), \quad (\text{A1})$$

$$\begin{aligned} G_{\psi \rightarrow \eta \gamma^*}(s) &= -\frac{4\sqrt{2}g_1}{3F}(a_1 - a_3) - \frac{16\sqrt{2}g_2}{3FM_\psi^2} [a_1 m_\pi^2 - a_3(2m_K^2 - m_\pi^2)] + \frac{4}{3} M_\psi \frac{F_V}{F} [(h_1 + 4h_2 \frac{m_\pi^2}{M_\psi^2} + 2h_3)a_1 \\ &\quad + h_3 a_3] D_\omega(s) - \frac{4}{3} M_\psi \frac{F_V}{F} \left\{ [h_1 + 4h_2 \frac{1}{M_\psi^2} (2m_K^2 - m_\pi^2) + h_3] a_3 + 2h_3 a_1 \right\} D_\phi(s) \\ &\quad + \lambda_{\eta\eta_c} g_{\psi\eta_c\gamma}(s) e^{i\delta_\eta}, \end{aligned} \quad (\text{A2})$$

$$\begin{aligned}
G_{\psi \rightarrow \eta' \gamma^*}(s) = & -\frac{4\sqrt{2}g_1}{3F}(a_2 - a_4) - \frac{16\sqrt{2}g_2}{3FM_\psi^2}[a_2m_\pi^2 - a_4(2m_K^2 - m_\pi^2)] + \frac{4}{3}M_\psi \frac{F_V}{F}[(h_1 + 4h_2 \frac{m_\pi^2}{M_\psi^2} + 2h_3)a_2 \\
& + h_3a_4]D_\omega(s) - \frac{4}{3}M_\psi \frac{F_V}{F}\left\{[h_1 + 4h_2 \frac{1}{M_\psi^2}(2m_K^2 - m_\pi^2) + h_3]a_4 + 2h_3a_2\right\}D_\phi(s) \\
& + \lambda_{\eta' \eta_c} g_{\psi \eta_c \gamma}(s) e^{i\delta_{\eta'}} ,
\end{aligned} \tag{A3}$$

where the definition of $D_R(s)$ is

$$D_R(s) = \frac{1}{M_R^2 - s - iM_R\Gamma_R(s)} . \tag{A4}$$

For the narrow-width resonances ω and ϕ , we use the constant widths in the numerical discussion.

For the ρ resonance, the energy dependent width is given by [30]

$$\Gamma_\rho(s) = \frac{sM_V}{96\pi F^2}[\sigma_\pi^3\theta(s - 4m_\pi^2) + \frac{1}{2}\sigma_K^3\theta(s - 4m_K^2)] , \tag{A5}$$

where $\sigma_P = \sqrt{1 - 4m_P^2/s}$ and $\theta(s)$ is the step function.

Appendix B: The form factors of $VP\gamma^*$

The various form factors $F_{VP\gamma^*}(s)$ from different processes have already been given in Ref. [30] and we show them below for the sake of completeness:

$$\begin{aligned}
F_{\rho\pi\gamma^*}(s) = & -\frac{2\sqrt{2}}{3F_\pi M_V M_\rho}[(\tilde{c}_1 + \tilde{c}_2 + 8\tilde{c}_3 - \tilde{c}_5)m_\pi^2 + (\tilde{c}_2 + \tilde{c}_5 - \tilde{c}_1 - 2\tilde{c}_6)M_\rho^2 + (\tilde{c}_1 - \tilde{c}_2 + \tilde{c}_5)s] \\
& + \frac{4F_V}{3F_\pi M_\rho}D_\omega(s)[(\tilde{d}_1 + 8\tilde{d}_2 - \tilde{d}_3)m_\pi^2 + \tilde{d}_3(M_\rho^2 + s)] ,
\end{aligned} \tag{B1}$$

$$\begin{aligned}
F_{\rho\eta\gamma^*}(s) = & -\frac{4}{M_V M_\rho F}a_1[M_\rho^2(\tilde{c}_2 - \tilde{c}_1 + \tilde{c}_5 - 2\tilde{c}_6) + m_\eta^2(\tilde{c}_2 + \tilde{c}_1 - \tilde{c}_5) + 8\tilde{c}_3m_\pi^2 \\
& + (\tilde{c}_1 - \tilde{c}_2 + \tilde{c}_5)s] + \frac{4\sqrt{2}F_V}{M_\rho F}D_\rho(s)a_1[\tilde{d}_3(M_\rho^2 - m_\eta^2 + s) + \tilde{d}_1m_\eta^2 + 8\tilde{d}_2m_\pi^2] \\
& - \frac{\sin\theta_8}{\cos(\theta_0 - \theta_8)F_0}\left[-\frac{4\sqrt{2}M_V}{M_\rho}\tilde{c}_8 + \frac{8F_V M_V^2}{M_\rho}\tilde{d}_5D_\rho(s)\right] ,
\end{aligned} \tag{B2}$$

$$\begin{aligned}
F_{\rho\eta'\gamma^*}(s) = & -\frac{4}{M_V M_\rho F}a_2[M_\rho^2(\tilde{c}_2 - \tilde{c}_1 + \tilde{c}_5 - 2\tilde{c}_6) + m_{\eta'}^2(\tilde{c}_2 + \tilde{c}_1 - \tilde{c}_5) + 8\tilde{c}_3m_\pi^2 \\
& + (\tilde{c}_1 - \tilde{c}_2 + \tilde{c}_5)s] + \frac{4\sqrt{2}F_V}{M_\rho F}D_\rho(s)a_2[\tilde{d}_3(M_\rho^2 - m_{\eta'}^2 + s) + \tilde{d}_1m_{\eta'}^2 + 8\tilde{d}_2m_\pi^2] \\
& - \frac{\cos\theta_8}{\cos(\theta_0 - \theta_8)F_0}\left[\frac{4\sqrt{2}M_V}{M_\rho}\tilde{c}_8 - \frac{8F_V M_V^2}{M_\rho}\tilde{d}_5D_\rho(s)\right] ,
\end{aligned} \tag{B3}$$

$$\begin{aligned}
F_{\omega\pi\gamma^*}(s) = & -\frac{2\sqrt{2}}{F_\pi M_V M_\omega} [(\tilde{c}_1 + \tilde{c}_2 + 8\tilde{c}_3 - \tilde{c}_5)m_\pi^2 + (\tilde{c}_2 + \tilde{c}_5 - \tilde{c}_1 - 2\tilde{c}_6)M_\omega^2 + (\tilde{c}_1 - \tilde{c}_2 + \tilde{c}_5)s] \\
& + \frac{4F_V}{F_\pi M_\omega} D_\rho(s) [(\tilde{d}_1 + 8\tilde{d}_2 - \tilde{d}_3)m_\pi^2 + \tilde{d}_3(M_\omega^2 + s)] + r_1 M_\omega D_{\rho'}(s), \tag{B4}
\end{aligned}$$

$$\begin{aligned}
F_{\omega\eta\gamma^*}(s) = & -\frac{4}{3M_V M_\omega F} a_1 [M_\omega^2(\tilde{c}_2 - \tilde{c}_1 + \tilde{c}_5 - 2\tilde{c}_6) + m_\eta^2(\tilde{c}_2 + \tilde{c}_1 - \tilde{c}_5) + 8\tilde{c}_3 m_\pi^2 \\
& + (\tilde{c}_1 - \tilde{c}_2 + \tilde{c}_5)s] + \frac{4\sqrt{2}F_V}{3M_\omega F} D_\omega(s) a_1 [\tilde{d}_3(M_\omega^2 - m_\eta^2 + s) + \tilde{d}_1 m_\eta^2 + 8\tilde{d}_2 m_\pi^2] \\
& - \frac{\sin \theta_8}{3 \cos(\theta_0 - \theta_8) F_0} \left[-\frac{4\sqrt{2}M_V}{M_\omega} \tilde{c}_8 + \frac{8F_V M_V^2}{M_\omega} \tilde{d}_5 D_\omega(s) \right], \tag{B5}
\end{aligned}$$

$$\begin{aligned}
F_{\omega\eta'\gamma^*}(s) = & -\frac{4}{3M_V M_\omega F} a_2 [M_\omega^2(\tilde{c}_2 - \tilde{c}_1 + \tilde{c}_5 - 2\tilde{c}_6) + m_{\eta'}^2(\tilde{c}_2 + \tilde{c}_1 - \tilde{c}_5) + 8\tilde{c}_3 m_\pi^2 \\
& + (\tilde{c}_1 - \tilde{c}_2 + \tilde{c}_5)s] + \frac{4\sqrt{2}F_V}{3M_\omega F} D_\omega(s) a_2 [\tilde{d}_3(M_\omega^2 - m_{\eta'}^2 + s) + \tilde{d}_1 m_{\eta'}^2 + 8\tilde{d}_2 m_\pi^2] \\
& - \frac{\cos \theta_8}{3 \cos(\theta_0 - \theta_8) F_0} \left[\frac{4\sqrt{2}M_V}{M_\omega} \tilde{c}_8 - \frac{8F_V M_V^2}{M_\omega} \tilde{d}_5 D_\omega(s) \right] \Big\}, \tag{B6}
\end{aligned}$$

$$\begin{aligned}
F_{\phi\eta\gamma^*}(s) = & -\frac{4\sqrt{2}}{3M_V M_\phi F} a_3 [M_\phi^2(\tilde{c}_2 - \tilde{c}_1 + \tilde{c}_5 - 2\tilde{c}_6) + m_\eta^2(\tilde{c}_2 + \tilde{c}_1 - \tilde{c}_5) + 8\tilde{c}_3(2m_K^2 - m_\pi^2) \\
& + (\tilde{c}_1 - \tilde{c}_2 + \tilde{c}_5)s] + \frac{8F_V}{3M_\phi F} D_\phi(s) a_3 [\tilde{d}_3(M_\phi^2 - m_\eta^2 + s) + \tilde{d}_1 m_\eta^2 + 8\tilde{d}_2(2m_K^2 - m_\pi^2)] \\
& - \frac{\sin \theta_8}{\cos(\theta_0 - \theta_8) F_0} \left[-\frac{8M_V}{3M_\phi} \tilde{c}_8 + \frac{8\sqrt{2}F_V M_V^2}{3M_\phi} \tilde{d}_5 D_\phi(s) \right], \tag{B7}
\end{aligned}$$

$$\begin{aligned}
F_{\phi\eta'\gamma^*}(s) = & -\frac{4\sqrt{2}}{3M_V M_\phi F} a_4 [M_\phi^2(\tilde{c}_2 - \tilde{c}_1 + \tilde{c}_5 - 2\tilde{c}_6) + m_{\eta'}^2(\tilde{c}_2 + \tilde{c}_1 - \tilde{c}_5) + 8\tilde{c}_3(2m_K^2 - m_\pi^2) \\
& + (\tilde{c}_1 - \tilde{c}_2 + \tilde{c}_5)s] + \frac{8F_V}{3M_\phi F} D_\phi(s) a_4 [\tilde{d}_3(M_\phi^2 - m_{\eta'}^2 + s) + \tilde{d}_1 m_{\eta'}^2 + 8\tilde{d}_2(2m_K^2 - m_\pi^2)] \\
& + \frac{\cos \theta_8}{\cos(\theta_0 - \theta_8) F_0} \left[-\frac{8M_V}{3M_\phi} \tilde{c}_8 + \frac{8\sqrt{2}F_V M_V^2}{3M_\phi} \tilde{d}_5 D_\phi(s) \right], \tag{B8}
\end{aligned}$$

$$\begin{aligned}
F_{K^{*+}K^-\gamma^*}(s) = & -\frac{2\sqrt{2}}{3F_K M_V M_{K^*}} [(\tilde{c}_1 + \tilde{c}_2 + 8\tilde{c}_3 - \tilde{c}_5)m_K^2 + (\tilde{c}_2 + \tilde{c}_5 - \tilde{c}_1 - 2\tilde{c}_6)M_{K^*}^2 + (\tilde{c}_1 - \tilde{c}_2 + \tilde{c}_5)s \\
& + 24\tilde{c}_4(m_K^2 - m_\pi^2)] + \frac{2F_V}{3F_K M_{K^*}} [(\tilde{d}_1 + 8\tilde{d}_2 - \tilde{d}_3)m_K^2 + \tilde{d}_3(M_{K^*}^2 + s)] \\
& [D_\omega(s) + 3D_\rho(s) - 2D_\phi(s)], \tag{B9}
\end{aligned}$$

$$F_{K^*0\bar{K}^0\gamma^*}(s) = \frac{4\sqrt{2}}{3F_K M_V M_{K^*}} [(\tilde{c}_1 + \tilde{c}_2 + 8\tilde{c}_3 - \tilde{c}_5)m_K^2 + (\tilde{c}_2 + \tilde{c}_5 - \tilde{c}_1 - 2\tilde{c}_6)M_{K^*}^2 + (\tilde{c}_1 - \tilde{c}_2 + \tilde{c}_5)s] \\ + \frac{2F_V}{3F_K M_{K^*}} [(\tilde{d}_1 + 8\tilde{d}_2 - \tilde{d}_3)m_K^2 + \tilde{d}_3(M_{K^*}^2 + s)] [D_\omega(s) - 3D_\rho(s) - 2D_\phi(s)]. \quad (\text{B10})$$

Appendix C: The form factors of $J/\psi \rightarrow VP$

The explicit expressions for the form factors of the $J/\psi \rightarrow VP$ defined in Eq. (30) are given below:

$$G_{\psi \rightarrow \rho^0 \pi^0} = \frac{2\sqrt{2}}{F_\pi M_\rho} h_1 M_\psi + \frac{8\sqrt{2}}{F_\pi M_\rho} h_2 m_\pi^2 \frac{1}{M_\psi} + \frac{32\pi\alpha}{F_\pi M_\rho} F_V g_1 + \frac{128\pi\alpha}{F_\pi M_\rho} F_V g_2 \frac{m_\pi^2}{M_\psi^2} + \frac{8\sqrt{2}\pi\alpha}{3} \frac{f_\psi}{M_\psi} F_{\rho\pi\gamma^*}(M_\psi^2), \quad (\text{C1})$$

$$G_{\psi \rightarrow \rho^+ \pi^-} = \frac{2\sqrt{2}}{F_\pi M_\rho} h_1 M_\psi + \frac{8\sqrt{2}}{F_\pi M_\rho} h_2 m_\pi^2 \frac{1}{M_\psi} + \frac{8\sqrt{2}\pi\alpha}{3} \frac{f_\psi}{M_\psi} F_{\rho\pi\gamma^*}(M_\psi^2), \quad (\text{C2})$$

$$G_{\psi \rightarrow \rho^0 \eta} = \frac{32\sqrt{2}\pi\alpha}{3F M_\rho} F_V g_1 (a_1 - a_3) + \frac{128\sqrt{2}\pi\alpha}{3F M_\rho M_\psi^2} F_V g_2 [a_1 m_\pi^2 - a_3 (2m_K^2 - m_\pi^2)] \\ - 8\pi\alpha \frac{F_V}{M_\rho} \lambda_{\eta\eta_c} g_{\psi\eta_c\gamma}(M_\rho^2) e^{i\delta_\eta} + \frac{8\sqrt{2}\pi\alpha}{3} \frac{f_\psi}{M_\psi} F_{\rho\eta\gamma^*}(M_\psi^2), \quad (\text{C3})$$

$$G_{\psi \rightarrow \rho^0 \eta'} = \frac{32\sqrt{2}\pi\alpha}{3F M_\rho} F_V g_1 (a_2 - a_4) + \frac{128\sqrt{2}\pi\alpha}{3F M_\rho M_\psi^2} F_V g_2 [a_2 m_\pi^2 - a_4 (2m_K^2 - m_\pi^2)] \\ - 8\pi\alpha \frac{F_V}{M_\rho} \lambda_{\eta'\eta_c} g_{\psi\eta_c\gamma}(M_\rho^2) e^{i\delta_{\eta'}} + \frac{8\sqrt{2}\pi\alpha}{3} \frac{f_\psi}{M_\psi} F_{\rho\eta'\gamma^*}(M_\psi^2), \quad (\text{C4})$$

$$G_{\psi \rightarrow \omega \pi^0} = \frac{32\pi\alpha}{3F_\pi M_\omega} F_V g_1 + \frac{128\pi\alpha}{3F_\pi M_\omega} F_V g_2 \frac{m_\pi^2}{M_\psi^2} + \frac{8\sqrt{2}\pi\alpha}{3} \frac{f_\psi}{M_\psi} F_{\omega\pi\gamma^*}(M_\psi^2), \quad (\text{C5})$$

$$G_{\psi \rightarrow \omega \eta} = \frac{4}{F M_\omega} a_1 h_1 M_\psi + \frac{16}{F M_\omega} a_1 h_2 m_\pi^2 \frac{1}{M_\psi} + \frac{4}{F M_\omega} (2a_1 + a_3) h_3 M_\psi + \frac{32\sqrt{2}\pi\alpha}{9F M_\omega} F_V g_1 (a_1 - a_3) \\ + \frac{128\sqrt{2}\pi\alpha}{9F M_\omega M_\psi^2} F_V g_2 [a_1 m_\pi^2 - a_3 (2m_K^2 - m_\pi^2)] - \frac{8}{3} \pi\alpha \frac{F_V}{M_\omega} \lambda_{\eta\eta_c} g_{\psi\eta_c\gamma}(M_\omega^2) e^{i\delta_\eta} \\ + \frac{8\sqrt{2}\pi\alpha}{3} \frac{f_\psi}{M_\psi} F_{\omega\eta\gamma^*}(M_\psi^2), \quad (\text{C6})$$

$$\begin{aligned}
G_{\psi \rightarrow \omega \eta'} = & \frac{4}{FM_\omega} a_2 h_1 M_\psi + \frac{16}{FM_\omega} a_2 h_2 m_\pi^2 \frac{1}{M_\psi} + \frac{4}{FM_\omega} (2a_2 + a_4) h_3 M_\psi + \frac{32\sqrt{2}\pi\alpha}{9FM_\omega} F_V g_1 (a_2 - a_4) \\
& + \frac{128\sqrt{2}\pi\alpha}{9FM_\omega M_\psi^2} F_V g_2 [a_2 m_\pi^2 - a_4 (2m_K^2 - m_\pi^2)] - \frac{8}{3} \pi\alpha \frac{F_V}{M_\omega} \lambda_{\eta' \eta_c} g_{\psi \eta_c \gamma} (M_\omega^2) e^{i\delta_{\eta'}} \\
& + \frac{8\sqrt{2}\pi\alpha}{3} \frac{f_\psi}{M_\psi} F_{\omega \eta' \gamma^*} (M_\psi^2), \tag{C7}
\end{aligned}$$

$$\begin{aligned}
G_{\psi \rightarrow \phi \eta} = & -\frac{2\sqrt{2}}{FM_\phi} a_3 h_1 M_\psi - \frac{8\sqrt{2}}{FM_\phi} a_3 h_2 (2m_K^2 - m_\pi^2) \frac{1}{M_\psi} - \frac{2\sqrt{2}}{FM_\phi} (2a_1 + a_3) h_3 M_\psi \\
& + \frac{64\pi\alpha}{9FM_\phi} F_V g_1 (a_1 - a_3) + \frac{256\pi\alpha}{9FM_\phi M_\psi^2} F_V g_2 [a_1 m_\pi^2 - a_3 (2m_K^2 - m_\pi^2)] \\
& - \frac{8\sqrt{2}}{3M_\phi} \pi\alpha F_V \lambda_{\eta \eta_c} g_{\psi \eta_c \gamma} (M_\phi^2) e^{i\delta_\eta} + \frac{8\sqrt{2}\pi\alpha}{3} \frac{f_\psi}{M_\psi} F_{\phi \eta \gamma^*} (M_\psi^2), \tag{C8}
\end{aligned}$$

$$\begin{aligned}
G_{\psi \rightarrow \phi \eta'} = & -\frac{2\sqrt{2}}{FM_\phi} a_4 h_1 M_\psi - \frac{8\sqrt{2}}{FM_\phi} a_4 h_2 (2m_K^2 - m_\pi^2) \frac{1}{M_\psi} - \frac{2\sqrt{2}}{FM_\phi} (2a_2 + a_4) h_3 M_\psi \\
& + \frac{64\pi\alpha}{9FM_\phi} F_V g_1 (a_2 - a_4) + \frac{256\pi\alpha}{9FM_\phi M_\psi^2} F_V g_2 [a_2 m_\pi^2 - a_4 (2m_K^2 - m_\pi^2)] \\
& - \frac{8\sqrt{2}}{3M_\phi} \pi\alpha F_V \lambda_{\eta' \eta_c} g_{\psi \eta_c \gamma} (M_\phi^2) e^{i\delta_{\eta'}} + \frac{8\sqrt{2}\pi\alpha}{3} \frac{f_\psi}{M_\psi} F_{\phi \eta' \gamma^*} (M_\psi^2), \tag{C9}
\end{aligned}$$

$$G_{\psi \rightarrow K^{*+} K^-} = \frac{2\sqrt{2}}{F_K M_{K^*}} h_1 M_\psi + \frac{8\sqrt{2}}{F_K M_{K^*}} h_2 m_K^2 \frac{1}{M_\psi} + \frac{8\sqrt{2}\pi\alpha}{3} \frac{f_\psi}{M_\psi} F_{K^{*+} K^- \gamma^*} (M_\psi^2), \tag{C10}$$

$$G_{\psi \rightarrow K^{*0} \bar{K}^0} = \frac{2\sqrt{2}}{F_K M_{K^*}} h_1 M_\psi + \frac{8\sqrt{2}}{F_K M_{K^*}} h_2 m_K^2 \frac{1}{M_\psi} + \frac{8\sqrt{2}\pi\alpha}{3} \frac{f_\psi}{M_\psi} F_{K^{*0} \bar{K}^0 \gamma^*} (M_\psi^2). \tag{C11}$$

-
- [1] A. Seiden, H. F. W. Sadrozinski and H. E. Haber, Phys. Rev. D **38**, 824 (1988).
[2] T. Feldmann, P. Kroll and B. Stech, Phys. Rev. D **58**, 114006 (1998).
[3] C. E. Thomas, J. High Energy Phys. **0710**, 026 (2007).
[4] V. A. Novikov, M. A. Shifman, A. I. Vainshtein, and V. I. Zakharov, Nucl. Phys. **B165**, 55 (1980).
[5] K. Kawarabayashi and N. Ohta, Nucl. Phys. B **175**, 477 (1980).
[6] F. J. Gilman and R. Kauffman, Phys. Rev. D **36**, 2761 (1987).
[7] K. T. Chao, Nucl. Phys. **B335**, 101 (1990).

- [8] R. Escribano and J.M. Frere, Phys. Lett. B **459**, 288 (1999).
- [9] R. Escribano and J. M. Frere, J. High Energy Phys. **0506**, 029 (2005).
- [10] P. Kroll, Mod. Phys. Lett. A **20**, 2667 (2005).
- [11] J. M. Gerard and E. Kou, Phys. Lett. B **616**, 85 (2005).
- [12] Q. Zhao, Phys. Lett. B **697**, 52 (2011).
- [13] J. Fu, H. B. Li, X. Qin, and M. Z. Yang, Mod. Phys. Lett. A **27**, 1250223 (2012).
- [14] H. E. Haber and J. Perrier, Phys. Rev. D **32**, 2961 (1985).
- [15] P. Ball, J. M. Frere and M. Tytgat, Phys. Lett. B **365**, 367 (1996).
- [16] A. Bramon, R. Escribano, and M. D. Scadron, Phys. Lett. B **403**, 339 (1997).
- [17] J. M. Gerard and J. Weyers, Phys. Lett. B **462**, 324 (1999).
- [18] Q. Zhao, G. Li, and C. H. Chang, Phys. Lett. B **645**, 173 (2007).
- [19] G. Li, Q. Zhao, and C. H. Chang, J. Phys. G **35**, 055002 (2008).
- [20] R. Escribano, Eur. Phys. J. **C 65**, 467 (2010).
- [21] G. t'Hooft, Nucl. Phys. **B72** (1974) 461; E. Witten, Nucl. Phys. **B156** (1979) 269; A. V. Manohar, arXiv: hep-ph/9802419.
- [22] J. Gasser and H. Leutwyler, Annals Phys. **158**, 142 (1984); J. Gasser and H. Leutwyler, Nucl. Phys. **B250**, 465 (1985).
- [23] G. Ecker, J. Gasser, A. Pich and E. de Rafael, Nucl. Phys. **B321**, 311 (1989).
- [24] Z. H. Guo and J. A. Oller, Phys. Rev. D **84**, 034005 (2011).
- [25] Z. H. Guo, J. A. Oller and J. Ruiz de Elvira, Phys. Rev. D **86**, 054006 (2012).
- [26] Z. -H. Guo and P. Roig, Phys. Rev. D **82** (2010) 113016.
- [27] M. Jamin, A. Pich, and J. Portoles, Phys. Lett. **B 640**, 176 (2006).
- [28] P. Roig and J. J. Sanz-Cillero, Phys. Lett. B **733** (2014) 158.
- [29] P. Roig, A. Guevara and G. L. Castro, Phys. Rev. D **89**, 073016 (2014).
- [30] Y. H. Chen, Z. H. Guo, H. Q. Zheng, Phys. Rev. D **85**, 054018 (2012).
- [31] Y. H. Chen, Z. H. Guo, H. Q. Zheng, Phys. Rev. D **90**, 034013 (2014).
- [32] D. Zhou, E. L. Cui, H. X. Chen, L. S. Geng and L. H. Zhu, arXiv:1409.0178 [hep-lat].
- [33] M. Ablikim *et al.* (BESIII Collaboration), Phys. Rev. D **89**, 092008 (2014).
- [34] K. A. Olive *et al.* [Particle Data Group Collaboration], Chin. Phys. C **38**, 090001 (2014).
- [35] F. J. Gilman and R. Kauffman, Phys. Rev. D **36**, 2761 (1987).
- [36] T. Feldmann and P. Kroll, Phys. Lett. B **413**, 410 (1997).
- [37] For the review see: T. Feldmann, Int. J. Mod. Phys. **A15**, 159 (2000).
- [38] G. Amelino-Camelia, *et al.*, Eur. Phys. J. **C68**, 619 (2010).
- [39] L. P. Gan, and A. Gasparian, PoS **CD09** (2009) 048. And also the contribution from M. Kunkel at HADRON 2011: <http://www.e18.ph.tum.de/bgrube/hadron2011Proceedings/proceedings.pdf>.
- [40] H. B. Li, J. Phys. **G36**, 085009 (2009).
- [41] H. Leutwyler, Nucl. Phys. Proc. Suppl. **64**, 223 (1998).

- [42] T. Feldmann, P. Kroll and B. Stech, Phys. Lett. B **449**, 339 (1999).
- [43] F. De Fazio and M.R. Pennington, J. High Energy Phys. **07**, 051 (2000).
- [44] M. Benayoun, L. DelBuono and H. B. O'Connell, Eur. Phys. J. **C 17**, 593 (2000).
- [45] J. L. Goity, A. M. Bernstein and B. R. Holstein, Phys. Rev. D **66**, 076014 (2002).
- [46] A. Bramon, R. Escribano, and M.D. Scadron, Phys. Lett. B **503**, 271 (2001).
- [47] T. N. Pham, Phys. Lett. B **694**, 129 (2010).
- [48] G. Ecker, J. Gasser, H. Leutwyler, A. Pich and E. de Rafael, Phys. Lett. B **223**, 425 (1989).
- [49] G. t'Hooft, Nucl. Phys. **B72**, 461 (1974); E. Witten, Nucl. Phys. **B156**, 269 (1979); S. Coleman and E. Witten, Phys. Rev. Lett. **45**, 100 (1980); G. Veneziano, Phys. Lett. B **95**, 90 (1980).
- [50] R. Kaiser and H. Leutwyler, Eur. Phys. J. **C 17**, 623 (2000).
- [51] P. Herrera-Siklody, J. I. Latorre, P. Pascual and J. Taron, Nucl. Phys. **B497**, 345 (1997).
- [52] M. Gell-Mann, R. J. Oakes, and B. Renner, Phys. Rev. **175**, 2195 (1986).
- [53] R. Kaiser and H. Leutwyler, arXiv: hep-ph/9806336.
- [54] V. Cirigliano, G. Ecker, H. Neufeld and A. Pich, JHEP **0306** (2003) 012.
- [55] Zhi-Hui Guo and J. J. Sanz-Cillero, Phys. Rev. D **79** (2009) 096006.
- [56] Z. -H. Guo and J. J. Sanz-Cillero, Phys. Rev. D **89** (2014) 094024.
- [57] P. D. Ruiz-Femenia, A. Pich, J. Portoles, JHEP **0307** (2003) 003.
- [58] K. Kampf and J. Novotny, Phys. Rev. D **84** (2011) 014036.
- [59] J. J. Dudek, R. G. Edwards, and D. G. Richards, Phys. Rev. D **73**, 074507 (2006).
- [60] Y. Chen *et al.* (CLQCD Collaboration), Phys. Rev. D **84**, 034503 (2011).
- [61] R. Arnaldi *et al.* (NA60 Collaboration), Phys. Lett. B **677**, 260 (2009).
- [62] G. Usai *et al.* (NA60 Collaboration), Nucl. Phys. **A855**, 189 (2011).
- [63] S. P. Schneider, B. Kubis, F. Niecknig, Phys. Rev. D **86**, 054013 (2012).
- [64] A. Etkin, *et al.*, Phys. Rev. D **25**, 1786 (1982).
- [65] B. Kubis and F. Niecknig, arXiv:1412.5385 [hep-ph].
- [66] J. L. Rosner, Phys. Rev. D **79**, 097301 (2009).
- [67] Lepton-G Coll. R. I. Dzhelyadin *et al.*, Phys. Lett. B **94**, 548 (1980).
- [68] Lepton-G Coll. R. I. Dzhelyadin *et al.*, Phys. Lett. B **88**, 379 (1979).
- [69] CELLO Coll. H.-J. Behrend *et al.*, Z. Phys. **C49**, 401 (1991).
- [70] M.N. Achasov *et al.*, Phys. Lett. B **504**, 275 (2001).
- [71] R. Arnaldi *et al.*, Phys. Lett. B **677**, 260 (2009).
- [72] TPC/ 2γ Coll. H. Aihara *et al.*, Phys. Rev. Lett. **64**, 172 (1990).
- [73] M. Acciarri *et al.*, Phys. Lett. B **418**, 399 (1998).
- [74] J. M. Gerard and A. Martini, Phys. Lett. B **730**, 264 (2014).